Aircraft Noise Simulation at DLR

Roland Ewert
DLR Institute of Aerodynamics and Flow Technology
Technical Acoustics

CEAA 2012, Svetlogorsk, Russia, 18.09.-23.09.2012

Outline

- Aeroacoustic problems tackled at DLR Braunschweig
- Overview of simulation approaches
- Surface integral methods
    - Fast Multipole BEM tool
    - Influence of simplified propagation physics
- Volume discretization approach
    - Direct noise computation (DNC)
    - RANS based modeling of AFN with stochastic sound sources
    - DGM for aeroacoustic simulations

Sources of exterior noise at aircraft

Re-Number of order 10mio!

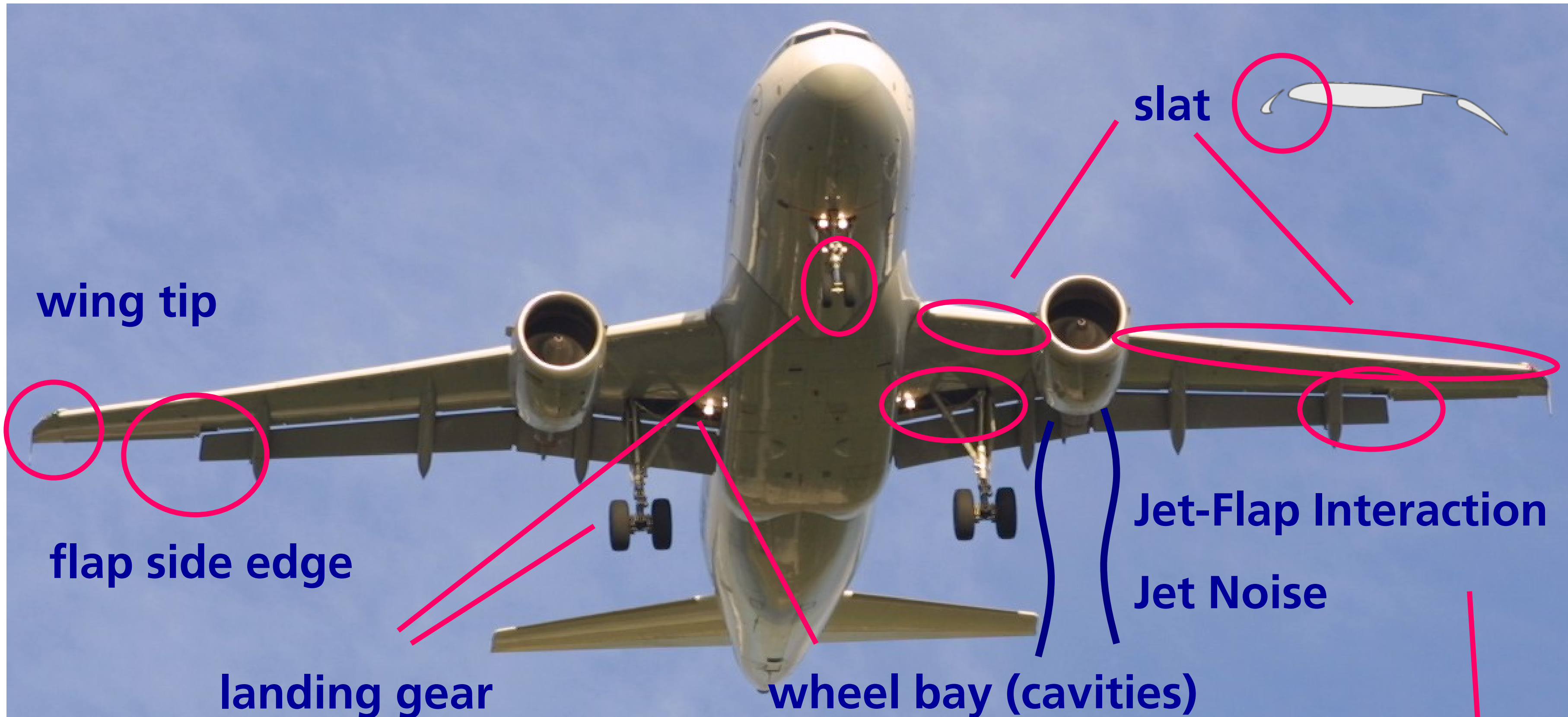

Sources of interior noise at aircraft

- **exterior excitation:**

airborne engine noise

fuselage boundary layer

- **interior excitation:**

air system

(hydraulic system)

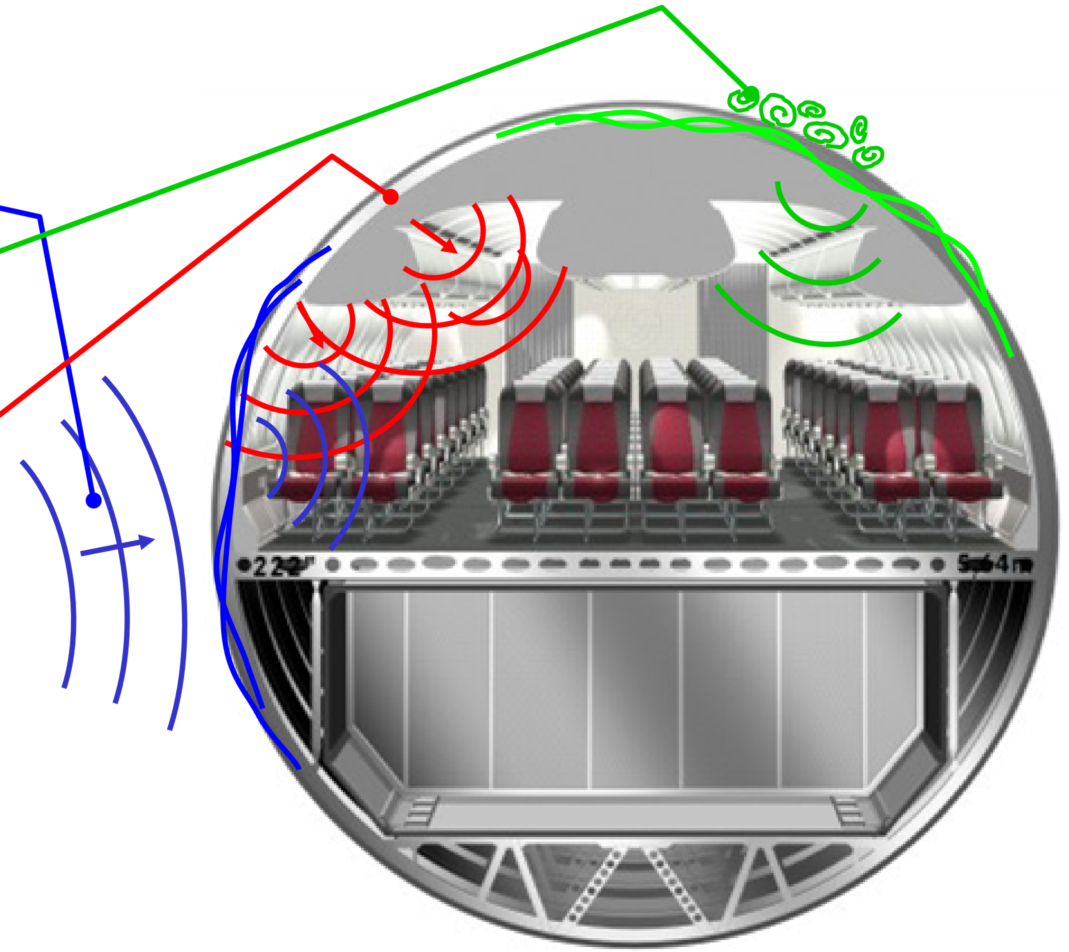

Aeroacoustic Simulation

Paths of simulations in Computational Aeroacoustics (CAA)

DLR FW-H Code APSIM+

DLR CAA Code PIANO

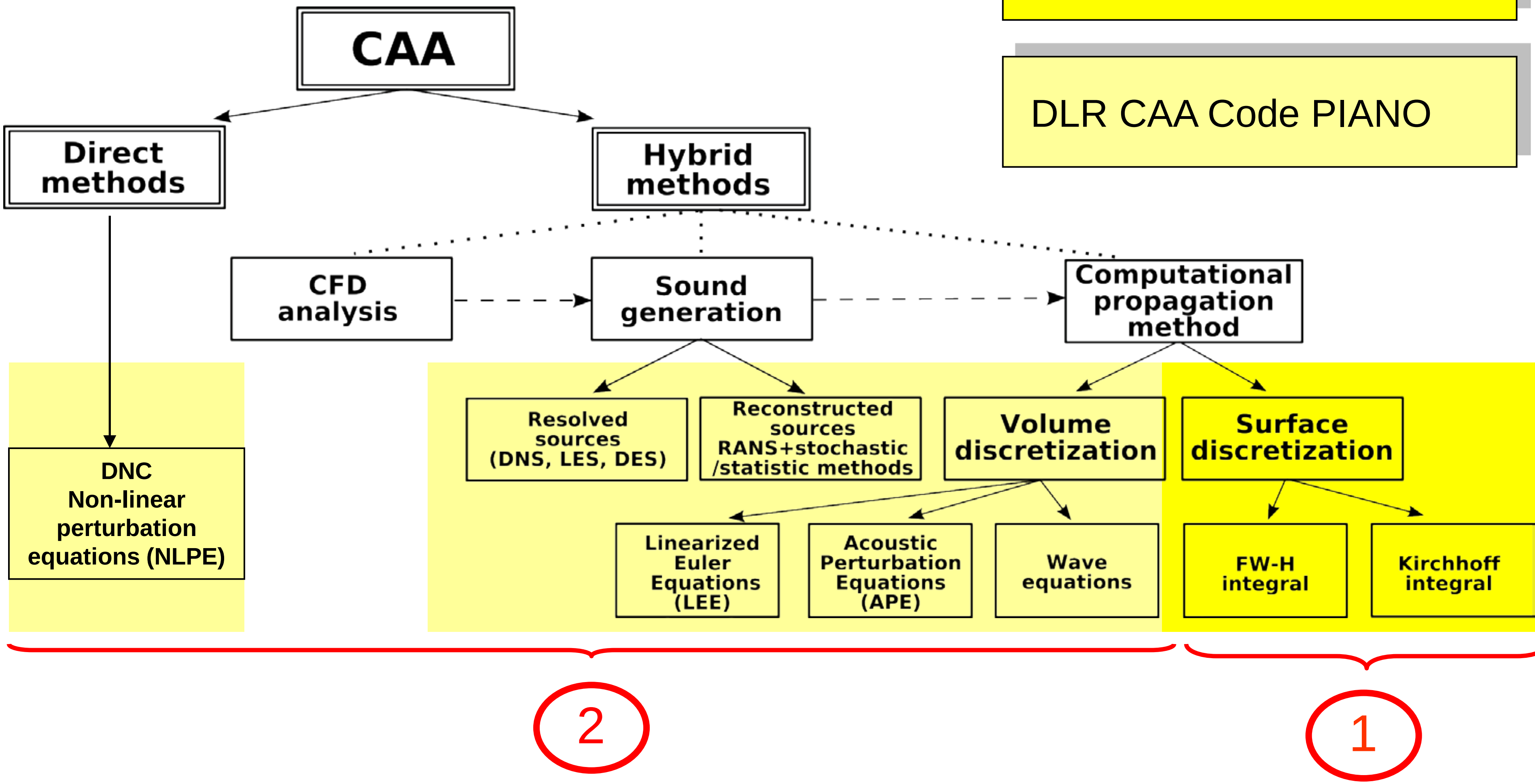

Volume discretization, moving medium

Simplified propagation physics

1

Tools for solution of wave equation

Direct propagation and acoustic installation

Source → **Interface model** → **Wave equation**

URANS/CAA
analyt.models

Direct: FW-H APSIM+
Installation:
Ray tracer SHADOW
Fast Multipole BEM

$\Rightarrow$ computation of acoustic installation + a/c farfield

Open rotor noise

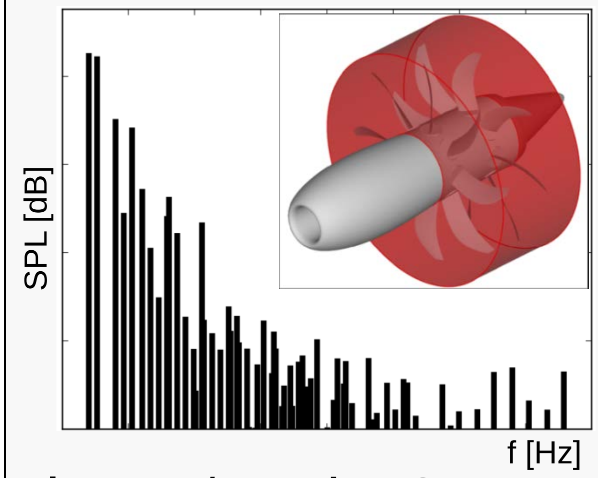

Flow: TAU/ sound: APSIM+

Acoustic a/c installation fan

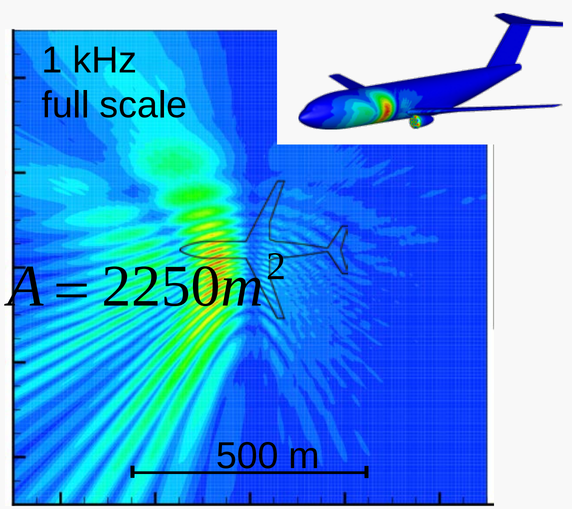

source: anal. (RRD)
sound: FM- BEM

Ultra fast installation estimation

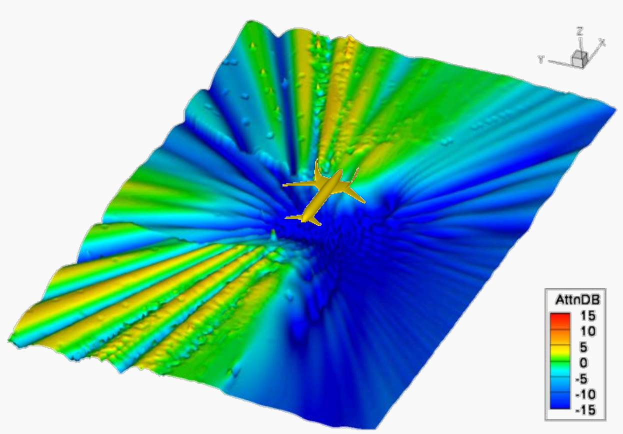

source: directed point source
noise: SHADOW

Acoustic a/c installation OR

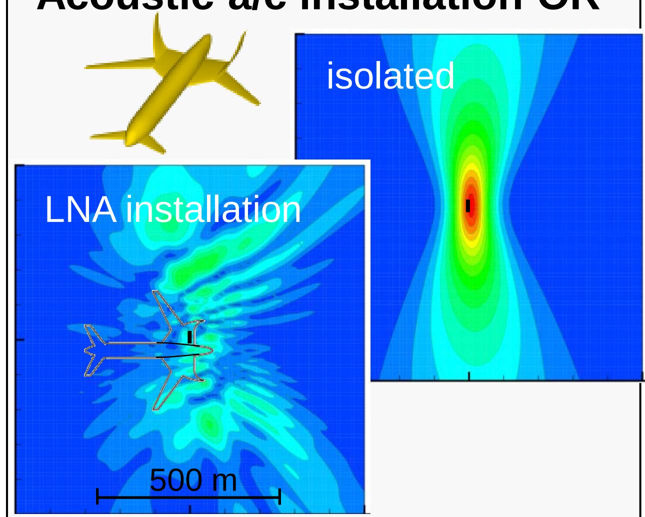

source: TAU fed analytical model
noise: FM-BEM

DLR

M. Lummer, M. Siefert, R. Akkermans

FW-H becomes FW-H + BEM if unsteady surface data is not available on the entire surface

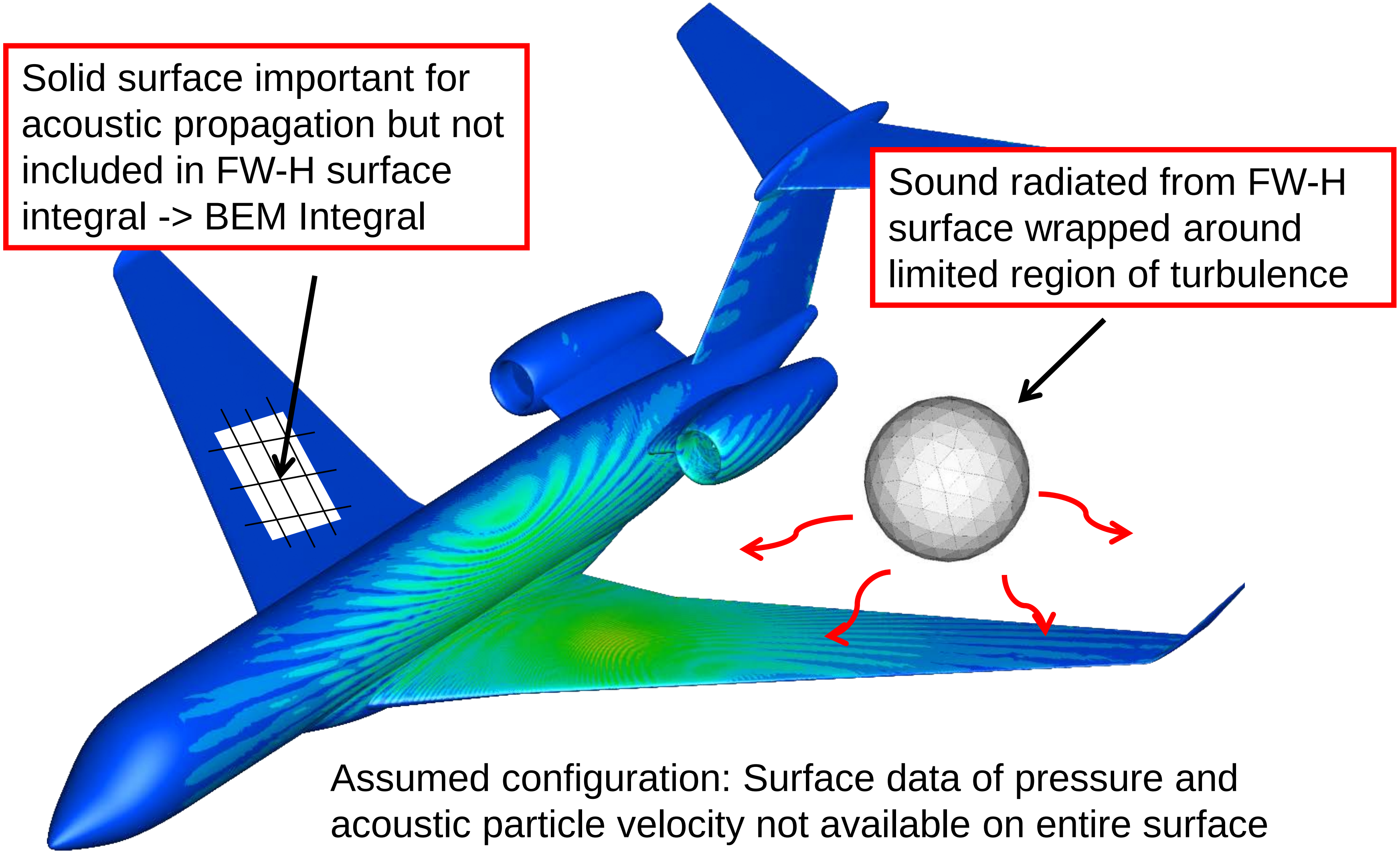

Assumed configuration: Surface data of pressure and acoustic particle velocity not available on entire surface

Boundary Element Method

- Solution of the (Helmholtz) wave equation
- Integral equation for the surface pressure: Burton/Miller formulation with wall admittance Y

$$[1+\alpha Y]\frac{p(x)}{2}-\int p(y)\left[1+\alpha\frac{\partial}{\partial n_x}\right]\left[\frac{\partial}{\partial n_y}-Y\right]G(x-y)d\Omega_y=\left[1+\alpha\frac{\partial}{\partial n_x}\right]p_{Inc}(x)$$

- Very large system of linear equations
  - Six elements per wave length necessary
- Direct solver (e.g. Gauss procedure)
  - Matrix is full, complex, and non-symmetric
  - Extremely expensive for higher frequencies (i.e. > 1 kHz)
- Iterative solver
  - No storage of matrix required
  - Fast matrix vector multiplication is necessary
  - Fast Multipole Method (FMM) is method of choice

Boundary Element Method - Memory

- 6 elements per wave length λ
- Number of triangle elements N, Surface A

$$N \approx 6^2 \frac{A}{\lambda^2}$$

- A340: $A \approx 2250 m^2$
- 341 Hz, $N \approx 8.1 \times 10^4$
- 2800 Hz, $N \approx 5.46 \times 10^6$
  - Matrix Elements: 2.982×10^{13}
  - Single precision storage: 2.385×10^{14} Bytes, ca. 240 TB Memory
  - Also working memory needed …
  - Tianhe-1A-NUDT (2 of TOP500) has about 230 TB Memory ...

Fast Multipole Method

- Iterative solution of BEM equation
- Acceleration of matrix-vector product from O(N^2) to O(N log(N))
  - Splitting of every row of product into near and far field terms
  - Calculation of far field interactions by a series expansion
  - Far field contributions are collected and distributed over an Octree covering the geometry
- Example: Full scale aircraft (surface 582 m^2)
  - 2170000 Triangles
  - Wavelength 0.1 m (3410 Hz)
  - 48 GB total memory (4 nodes)
  - 150s for one iteration step on 32 cores (Opteron 2.7 GHz)
  - 200 iteration steps (conjugate residual method)

CROR acoustic installation effects configuration studies

conventional a/c

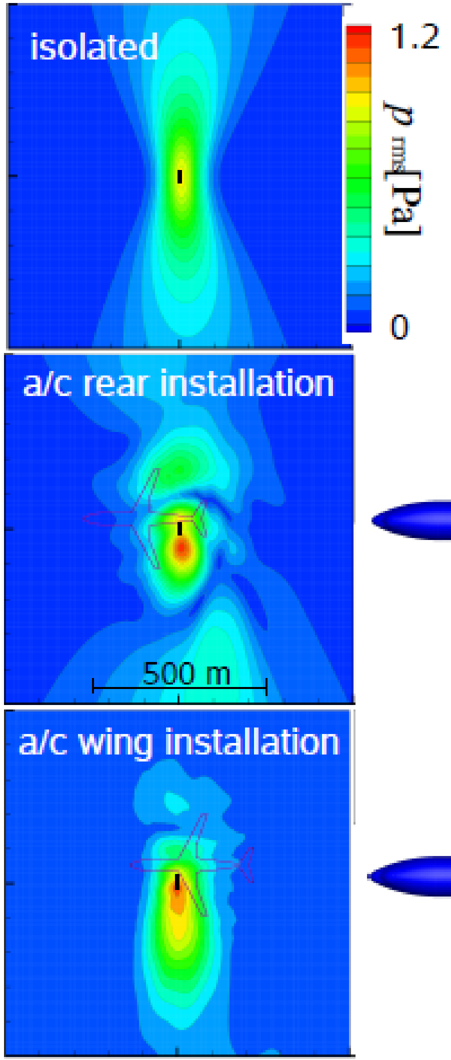

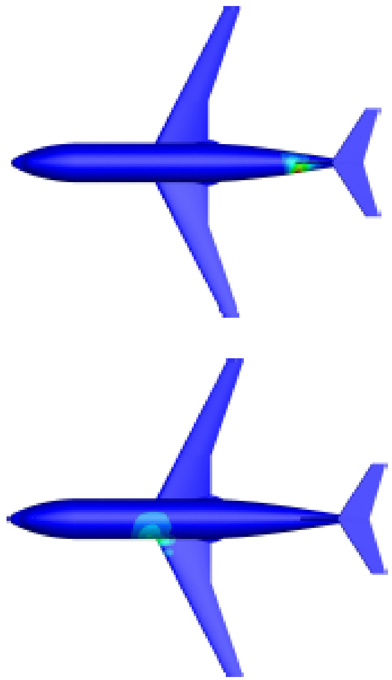

3 dB **increase**

Footprints of loading noise 120m below a/c for BPF of front rotor

Flow →

DLR Lna/c

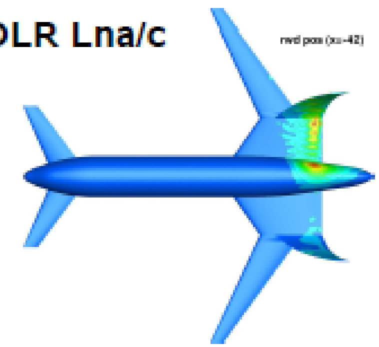

DLR Lna/c

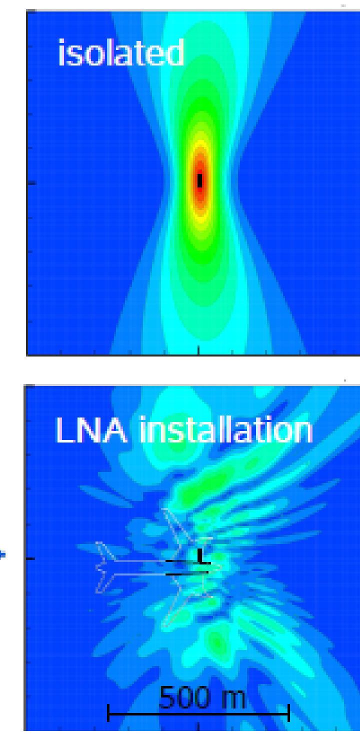

10-12 dB **reduction**

Source: uRANS
Sound: FMM BEM

F6OR Configuration
Front rotor installation effect

- 50,000 Surface Triangles
- FMM + CROR Model

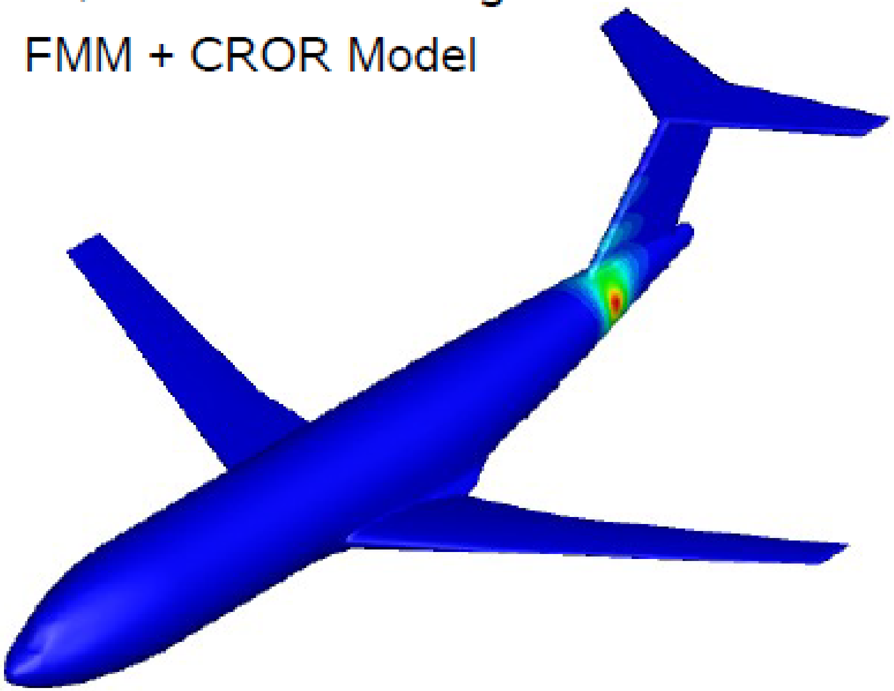

$B_f=10$

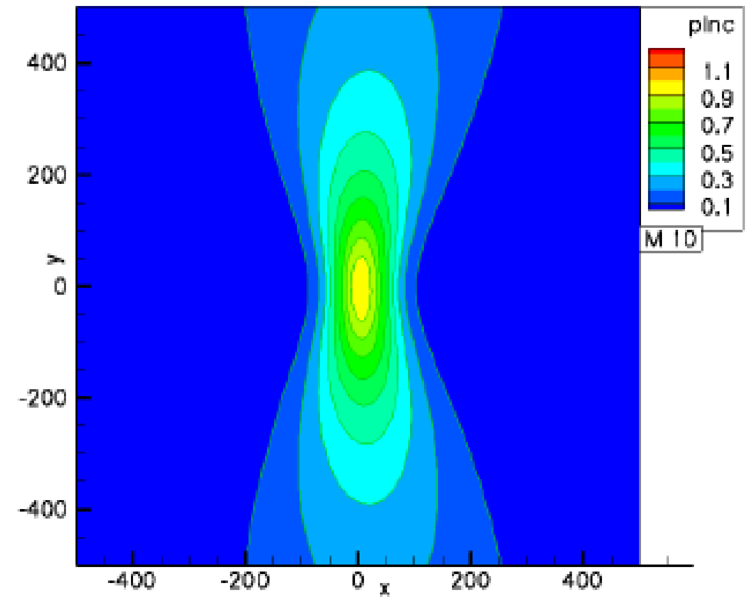

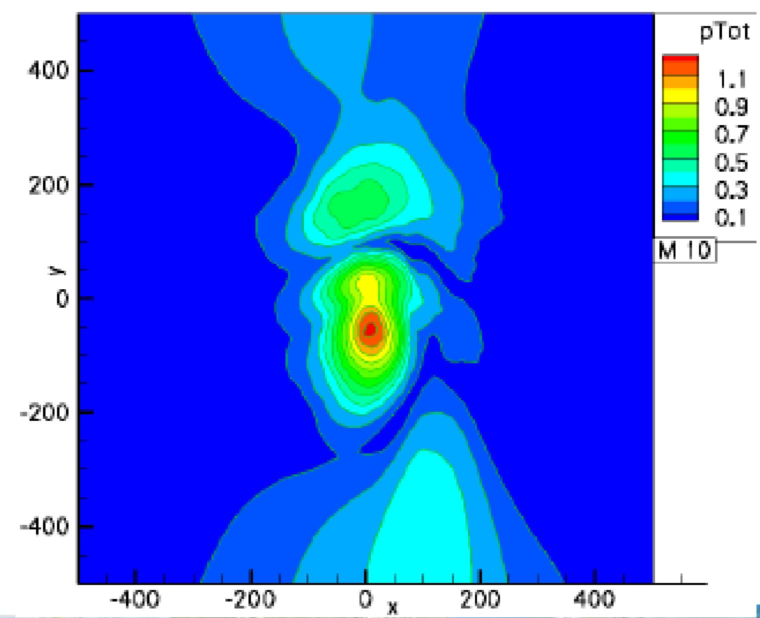

Source: uRANS
Sound: FMM BEM

1

F6OR Configuration
Interaction Harmonics

- 50,000 Surface Triangles
- FMM + CROR Model

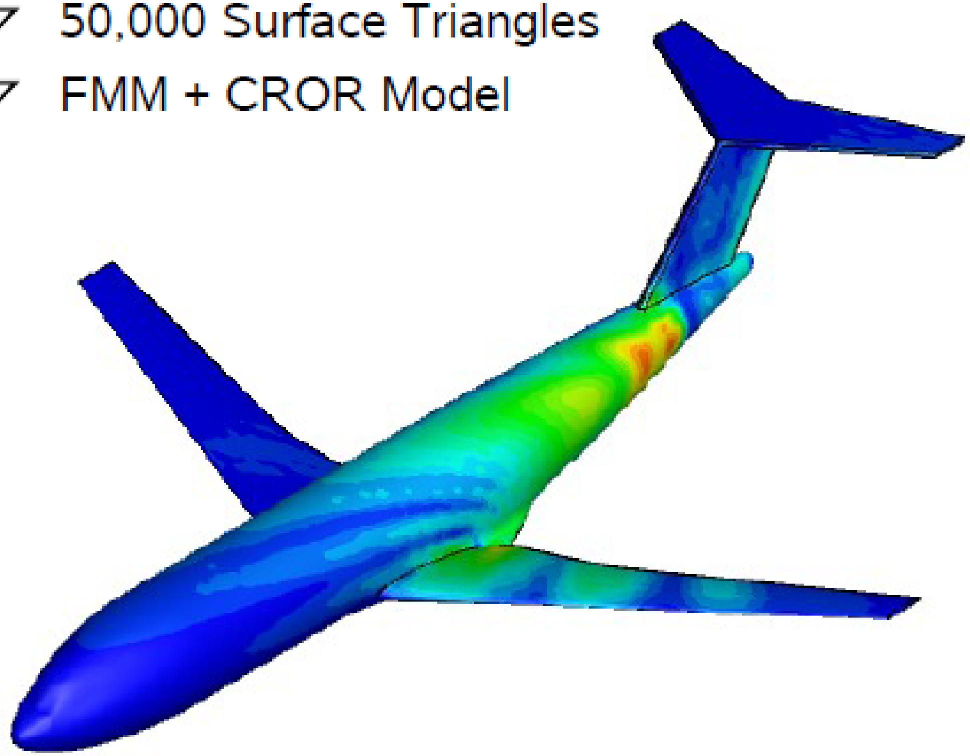

$B_f + B_a = 18$

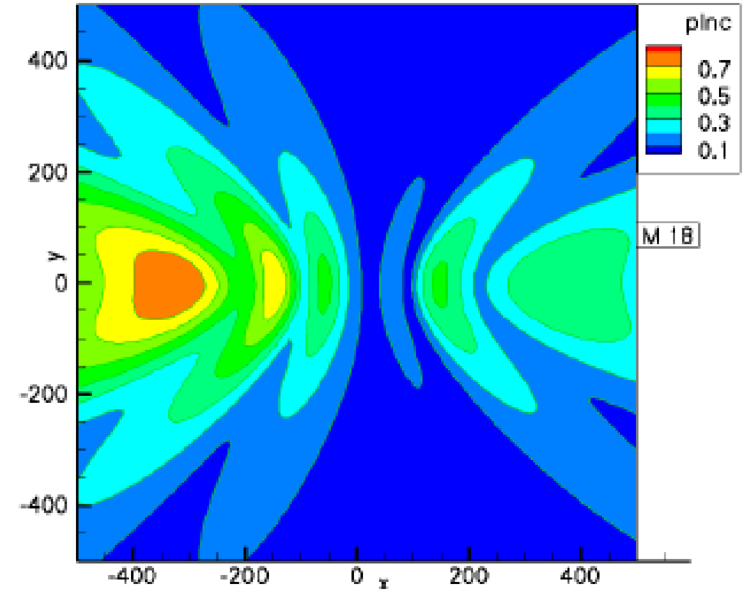

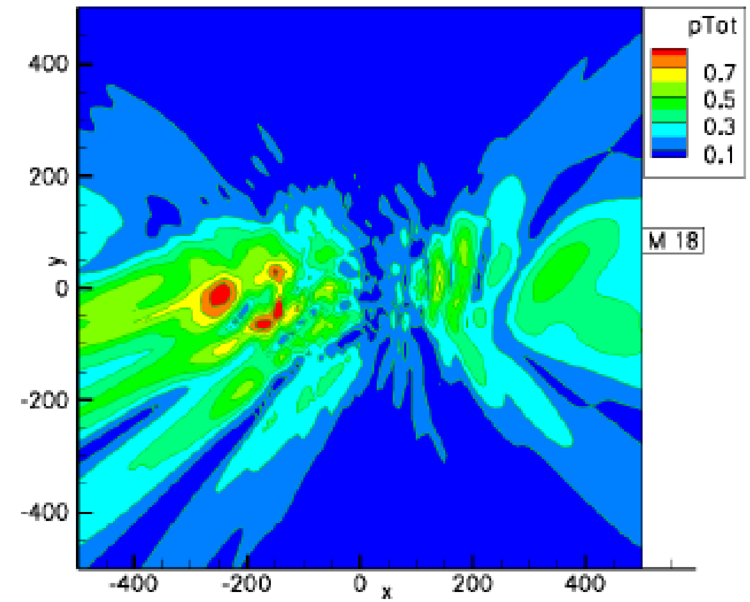

Source: uRANS
Sound: FMM BEM

Importance of acoustic propagation effects

Installation effect on fan tones at High Lift Wing

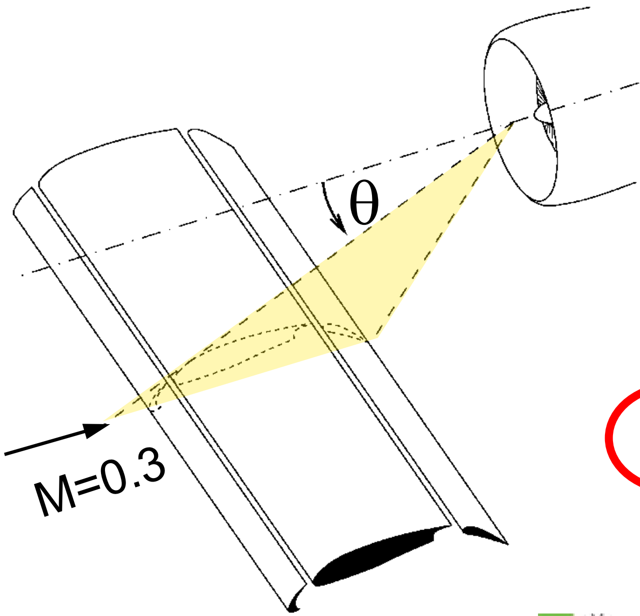

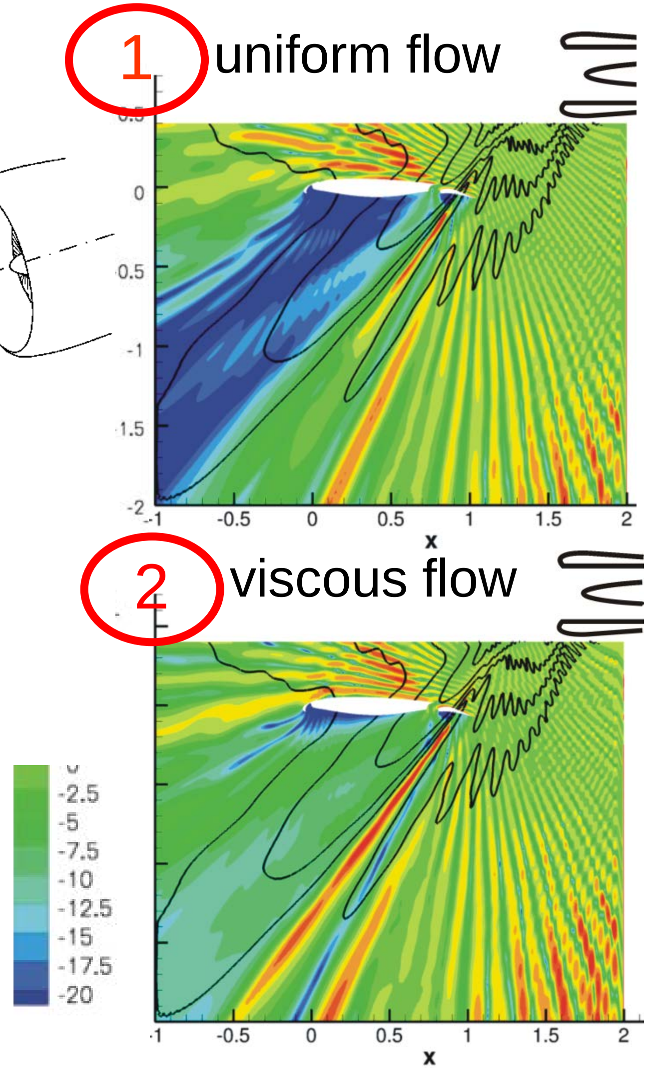

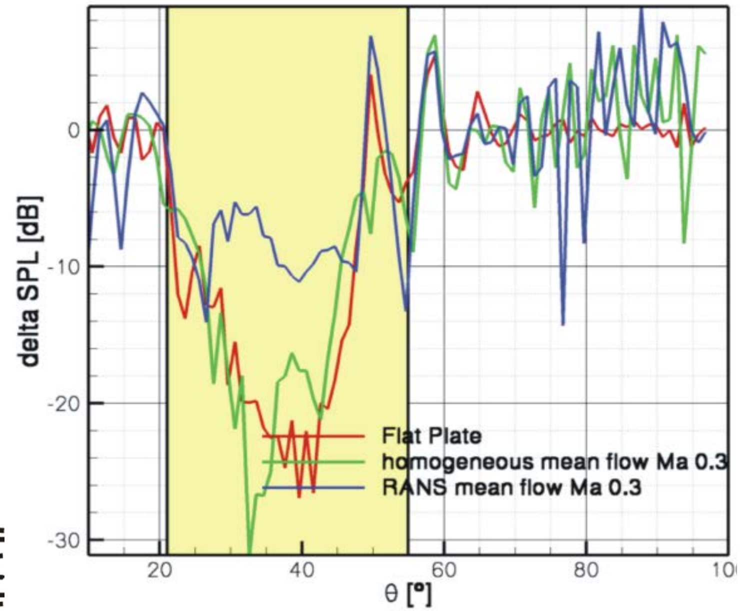

Simplified flow assumption overpredicts shielding by 10dB!

Strong viscous flow effects on noise shielding even at low M

(experience from EU project NACRE)

DLR

Slat Noise Simulations

Extension to unstructured CAA, 30P30N high-lift airfoil

2

- PIANO code of DLR based on structured multi-block (SMB) meshes + finite differences
- Dispersion Relation Preserving (DRP) scheme (Tam & Webb 1993)
- LEE, APE, NLEE, NLPE

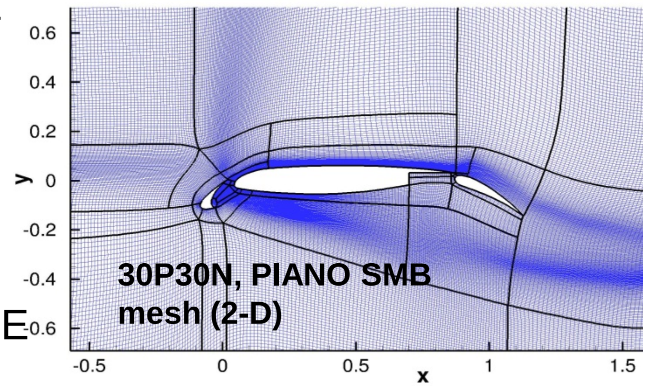

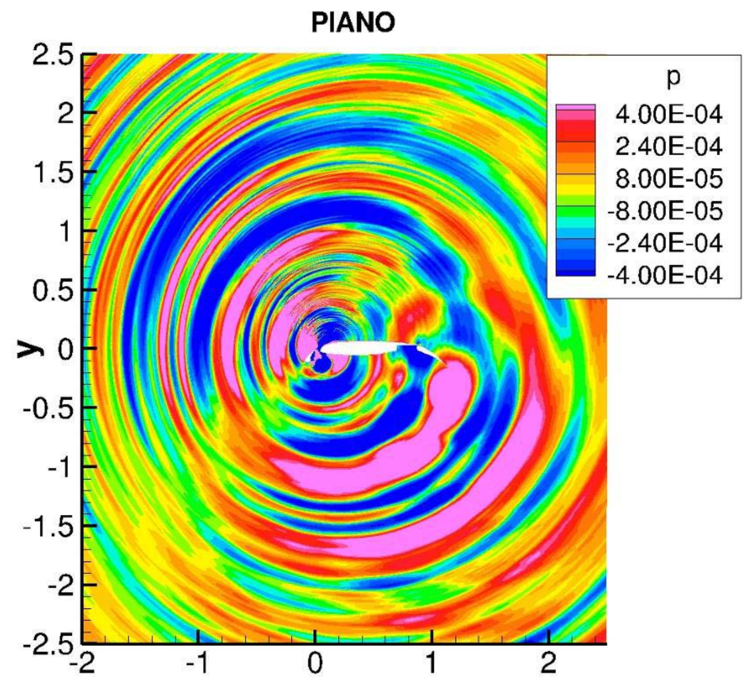

- Simplified mesh generation based on unstructured meshes with high-order methods
- Discontinuous Galerkin methods for CAA (Bauer et al. 2011
- LEE and APE

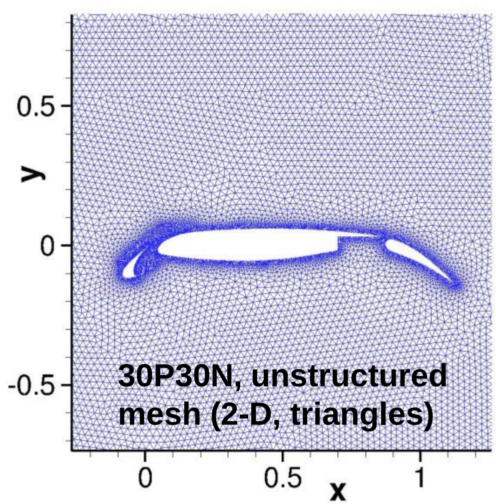

Disco (DGM)
M. Bauer et al., 2011

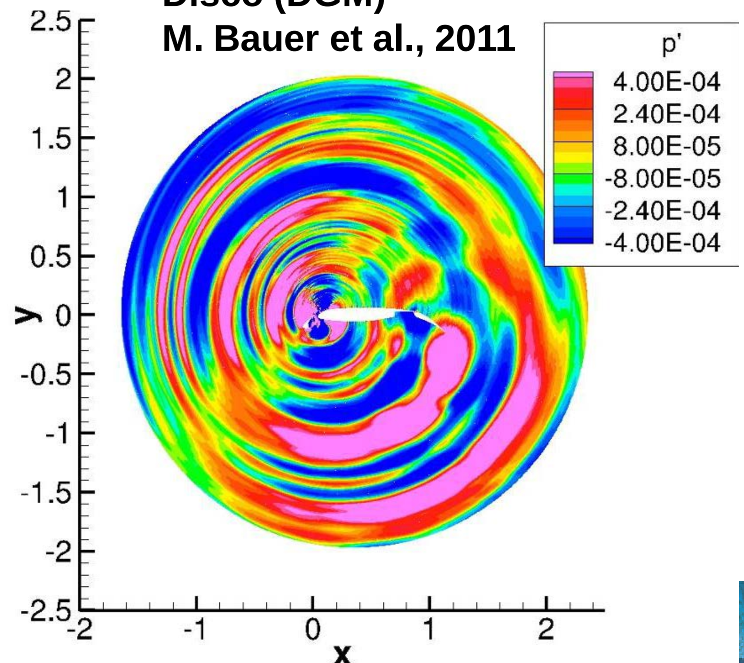

DLR

Governing equations

- **Navier-Stokes equations in primitive variable notations**

$$\begin{aligned} \frac{\partial \rho}{\partial t} + \nabla \cdot (\rho \boldsymbol{v}) &= 0\,, \\ \frac{\partial \boldsymbol{v}}{\partial t} + (\boldsymbol{v} \cdot \nabla)\boldsymbol{v} + \frac{\nabla p}{\rho} &= \frac{\nabla \cdot \boldsymbol{\tau}}{\rho}\,, \\ \frac{\partial p}{\partial t} + \boldsymbol{v} \cdot \nabla p + \gamma p \nabla \cdot \boldsymbol{v} &= (\gamma - 1)(\boldsymbol{\tau} \cdot \nabla) \cdot \boldsymbol{v} - (\gamma - 1)\nabla \cdot \mathbf{q}\,. \end{aligned}$$

Flow field decomposition into a steady and fluctuating part

$$\rho = \rho^0 + \rho', \quad \boldsymbol{v} = \boldsymbol{v}^0 + \boldsymbol{v}', \quad p = p^0 + p', \quad \boldsymbol{\tau} = \boldsymbol{\tau}^0 + \boldsymbol{\tau}', \quad \mathbf{q} = \mathbf{q}^0 + \mathbf{q}'\,.$$

Structured CAA Code PIANO

Development of Direct Noise Computation (DNC) capability

2

- **Viscous PENNE(*) equations with steady base flow ("NLPE") (**)**

$$
\frac{\partial \rho'}{\partial t} + \boldsymbol{v} \cdot \nabla \rho' + \boldsymbol{v}' \cdot \nabla \rho^0 + \rho \nabla \cdot \boldsymbol{v}' + \rho' \nabla \cdot \boldsymbol{v}^0 = r_1^0 ,
$$

$$
\frac{\partial \boldsymbol{v}'}{\partial t} + (\boldsymbol{v} \cdot \nabla)\boldsymbol{v}' + (\boldsymbol{v}' \cdot \nabla)\boldsymbol{v}^0 + \frac{\rho'}{\rho}(\boldsymbol{v}^0 \cdot \nabla)\boldsymbol{v}^0 + \frac{\nabla p'}{\rho} = \frac{\nabla \cdot \boldsymbol{\tau}'}{\rho} + \frac{\rho^0}{\rho}\boldsymbol{r}_2^0 ,
$$

$$
\frac{\partial p'}{\partial t} + \boldsymbol{v} \cdot \nabla p' + \boldsymbol{v}' \cdot \nabla p^0 + \gamma p \nabla \cdot \boldsymbol{v}' + \gamma p' \nabla \cdot \boldsymbol{v}^0 =
$$

$$
(\gamma - 1)\left[(\boldsymbol{\tau}' \cdot \nabla) \cdot \boldsymbol{v} + (\boldsymbol{\tau}^0 \cdot \nabla) \cdot \boldsymbol{v}' - \nabla \cdot \mathbf{q}'\right] + r_3^0 .
$$

with residual turbulent viscous and heat fluxes

$$
\begin{aligned}
r_1^0 &= 0 , \\
\boldsymbol{r}_2^0 &= -\frac{\nabla \cdot \boldsymbol{\tau}^{t0}}{\rho^0} , \\
r_3^0 &= -(\gamma - 1)\left[(\boldsymbol{\tau}^{t0} \cdot \nabla) \cdot \boldsymbol{v}^0 - \nabla \cdot \mathbf{q}^{t0}\right] .
\end{aligned}
$$

(*) PENNE = Perturbed Nonconnservative Nonlinear Equations, L. N. Long. *AIAA Paper 2000-1998*, 2000.

(**) primitive variables approach of NLDE (Morris et al., JCP 133, 1997; Terracol, Flow, Turb. & Comb, 77, 2006)

DLR

Structured CAA Code PIANO

Development of Direct Noise Computation (DNC) capability

2

Realized via 3 ghost values of $\boldsymbol{\sigma}$ on ghost points beneath wall

- **No-slip boundary condition**

Physics requires: $v_{wall} = 0$

Introducing $\sigma = \tau - pI$ into momentum equations of Navier-Stokes equations yields

$$\frac{\partial v}{\partial t} + (v \cdot \nabla) v = \frac{\nabla \cdot \boldsymbol{\sigma}}{\rho} .$$

To satisfy $\frac{\partial v}{\partial t} \stackrel{!}{=} 0$, $\boxed{\nabla \cdot \boldsymbol{\sigma} \stackrel{!}{=} 0}$

For viscous PENNE equations:

$$\sigma'_{ij} = \tau'_{ij} - p' \delta_{ij}$$

$u^0 = v^0 = w^0 = 0$ (from RANS background flow simulation)

$u' = v' = w' = 0$ (to be enforced at end of each time step)

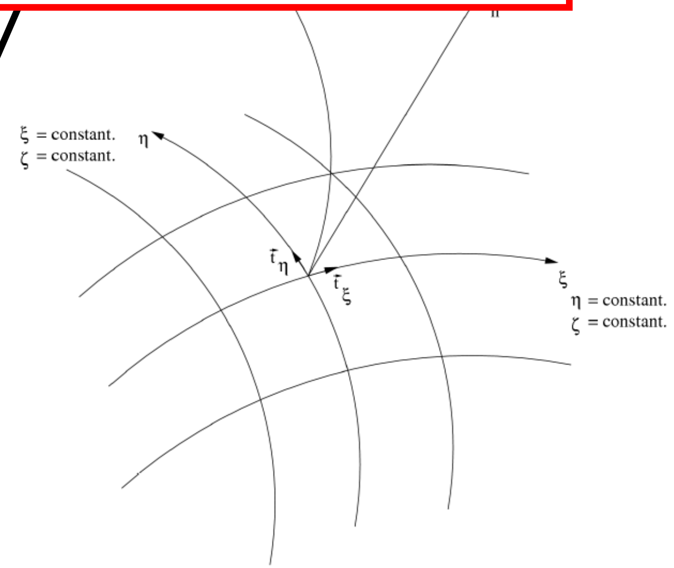

Fig. 3 Sketch of curvilinear coordinates w.r.t. wall boundary of a body fitted grid.

- **Adiabatic boundary condition**

For an adiabatic wall, heat flux through the wall must be zero, i.e.

$$\vec{q} \cdot \vec{n} \;=\; 0\,.$$

The thermal equation of state reads

$$\frac{dp}{p} - \frac{d\rho}{\rho} \;=\; \frac{dT}{T}\,.$$

After decomposition and rearrangement

$$\frac{\partial \rho'}{\partial n} \;=\; n_j \frac{\partial \rho'}{\partial x_j} \;=\; -n_j \left[-\frac{\rho}{p}\frac{\partial p'}{\partial x_j} - \frac{\rho'}{p}\frac{\partial p^0}{\partial x_j} + \frac{p'}{p}\frac{\partial \rho^0}{\partial x_j} \right],$$

$$\rho'_{i,-1,k} \;=\; \frac{1}{c_0}\left\{ -\sum_{m=0}^{5} c_{m+1}\rho'_{i,m,k} + \left[\frac{\partial \rho'}{\partial n} - \sum_{l=1}^{3} n_l \left(J_{1l}\frac{\partial \rho'}{\partial \xi} + J_{3l}\frac{\partial \rho'}{\partial \zeta} \right) \right] \Big/ \sum_{l=1}^{3} n_l J_{2l} \right\}.$$

Structured CAA Code PIANO

Development of Direct Noise Computation (DNC) capability

2

CAA simulation of flow around a circular cylinder, Re=150, M=0.1, 0.2, and 0.3(*)

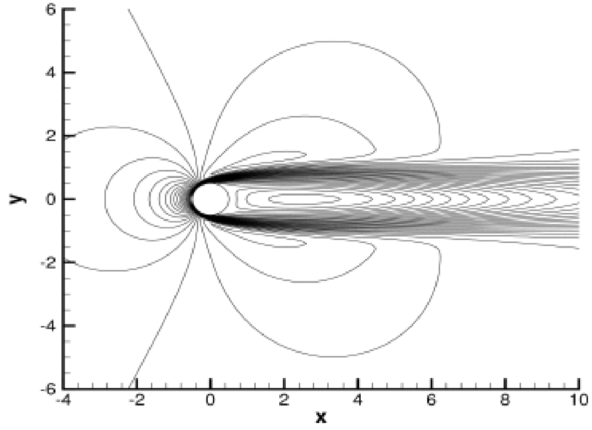

a) Base flow x-velocity u^0 from TAU RANS.

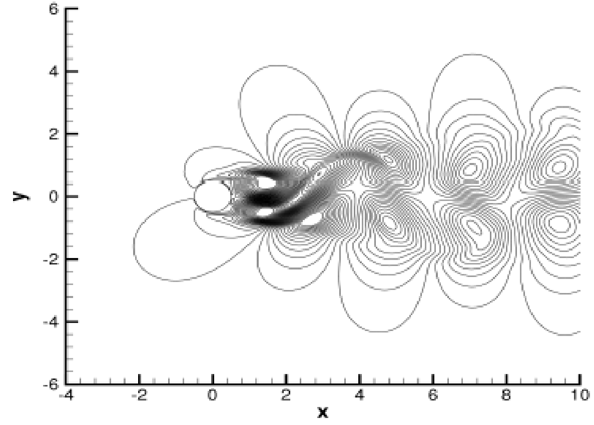

a) Fluctuating x-velocity $u' - \overline{u'}$.

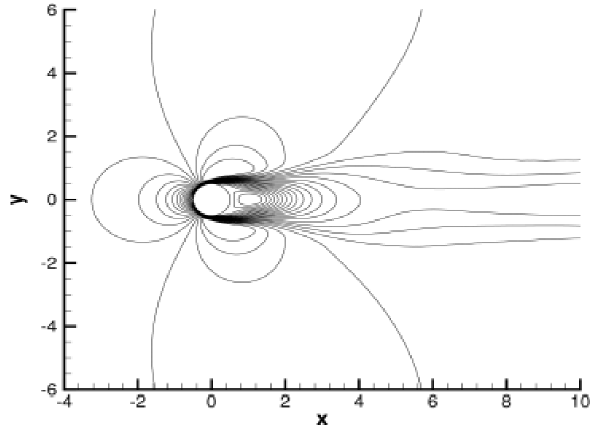

b) Mean x-velocity $u^0 + \overline{u'}$ with added mean contribution from PIANO.

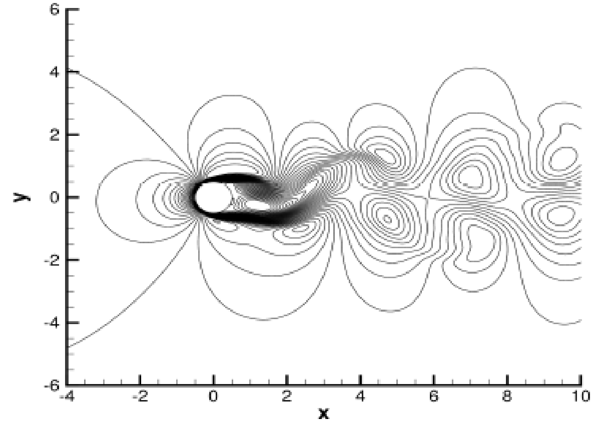

b) Total x-velocity $u^0 + u'$.

Base and mean-flow contour lines. Fluctuating and total-flow contour lines.

(*) O. Inoue and. N. Hatakeyama, *JFM*, Vol(471):285–314, 2002.

DLR

Structured CAA Code PIANO

Development of Direct Noise Computation (DNC) capability

Numerical verification for circular cylinder simulation

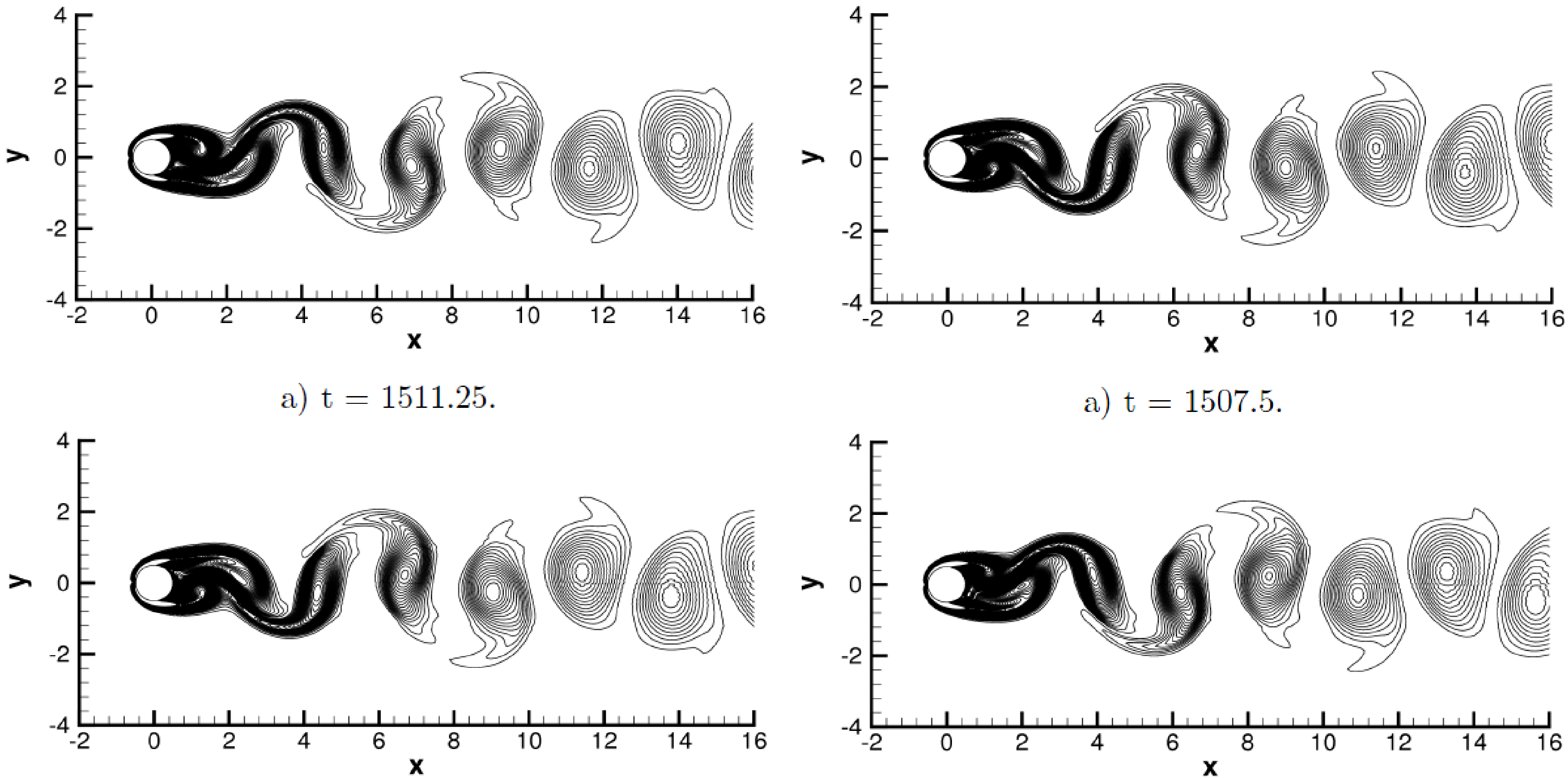

a) t = 1511.25.

a) t = 1507.5.

b) t = 1526.25.

b) t = 1511.25.

Time development of vorticity filed for Re = 150, M = 0.2 (left), M = 0.3 (right).

Structured CAA Code PIANO

Development of Direct Noise Computation (DNC) capability

2

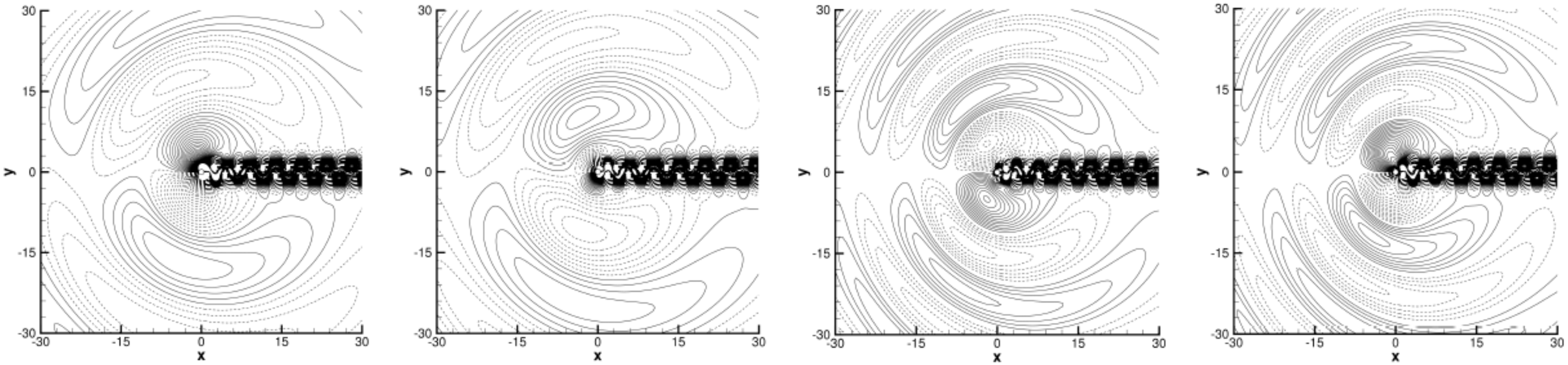

a) t=1702.5. b) t=1710. a) t=1702.5. b) t=1710.

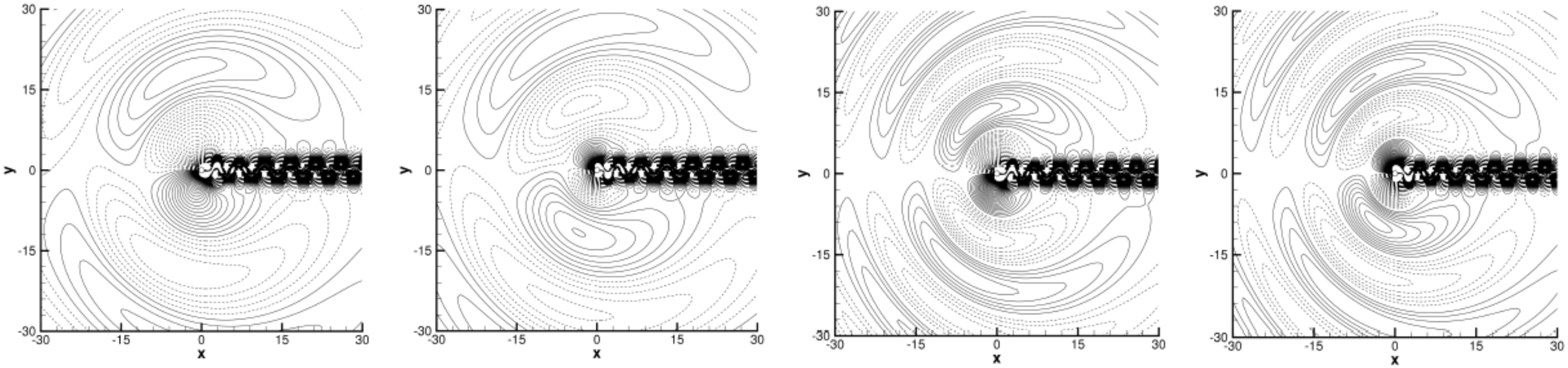

c) t=1717.5. d) t=1725. c) t=1717.5. d) t=1725.

Time development of pressure fluctuation for Re = 150, M = 0.2 (left), M = 0.3 (right), St=0.176 (M=0.1), St=0.185 (M=0.2), St=0.190 (M=0.3) (Inoue: M=0.2, St=0.185)

.

DLR

2

CAA simulation of flow around a circular cylinder

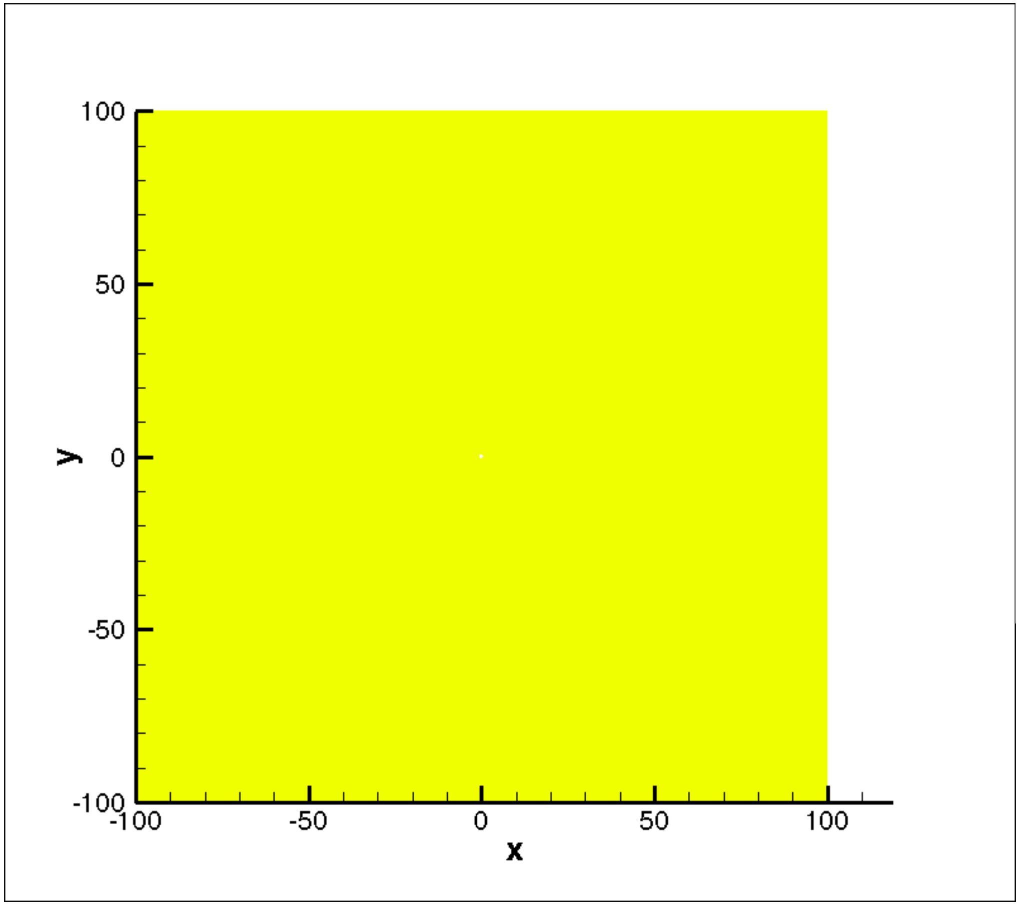

Time development of pressure fluctuation for
Re = 150, M = 0.2

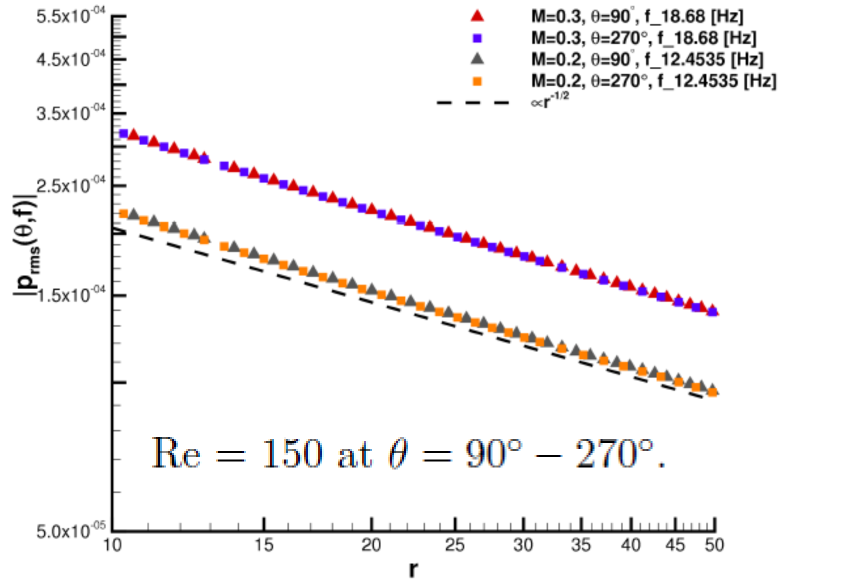

Decay of pressure peaks for M = 0.2-0.3,

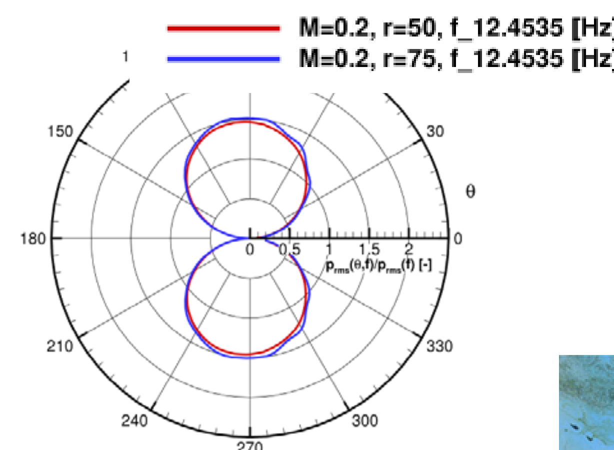

DLR

General motivation of stochastic noise modeling

Estimation of computational cost for A380 take-off/landing configuration

Attached boundary layer flow with separation on flap of a wing at high-lift „approximated“ by flow over a backward facing step.

LES with wall-functions

Surface: 0.38m x 0.05m

Cost: 10^6s on single CPU (= 20days)

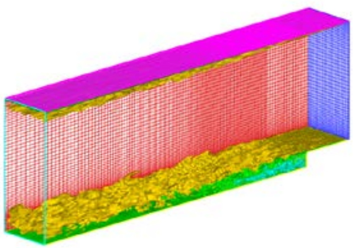

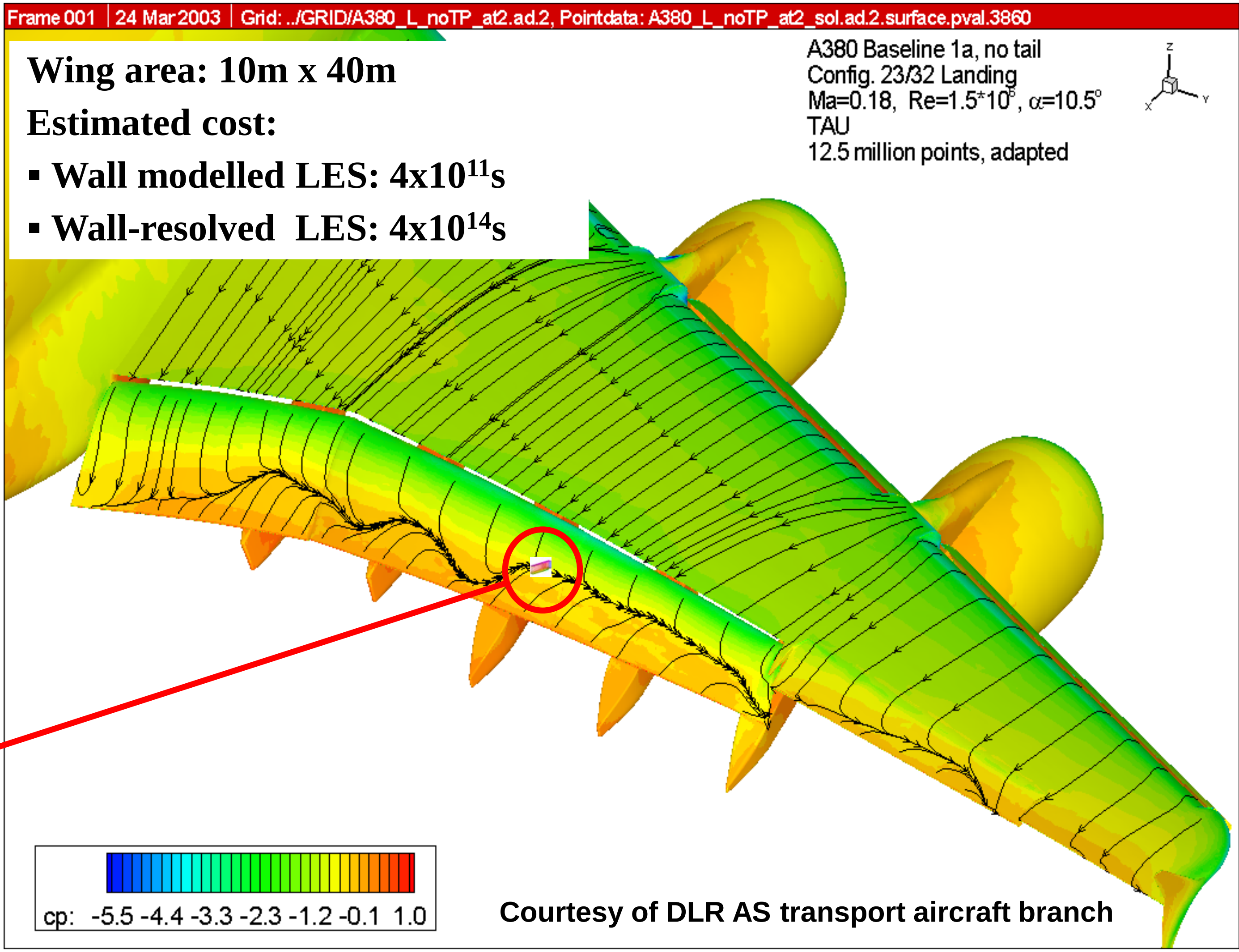

DLR

Tobias Knopp

General motivation of stochastic noise modeling

Need for fast design-to-noise simulation tools for turbulence related noise generation

- Tools need for the fast simulation of turbulence related broadband noise (BBN) for aeroacoustic design purposes (design-to-noise) in an industrial environment
- Short turnaround times needed
- 'First principle based method' needed, which is applicable to small standard variations but also to new designs
- Reynolds Averaged Navier-Stokes (RANS) equations standard tool in aerodynamics today
- Scale resolving simulation (DNC, DNS, LES, DES+FW-H) useful to study noise and understand new noise source mechanism but still too expensive for aeroacoustic design purposes today and in the near future
- In the meantime need for a RANS equivalent in CAA for BBN predictions

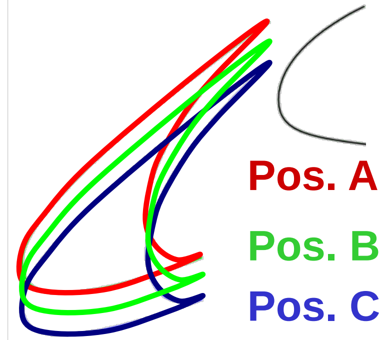

Example: slat setting variation: impact on aerodynamics and <u>noise</u>

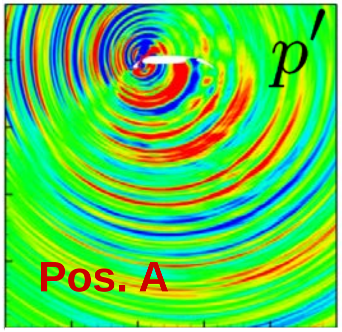

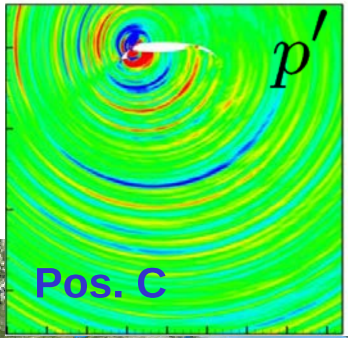

DLR

Stochastic noise prediction methods at DLR

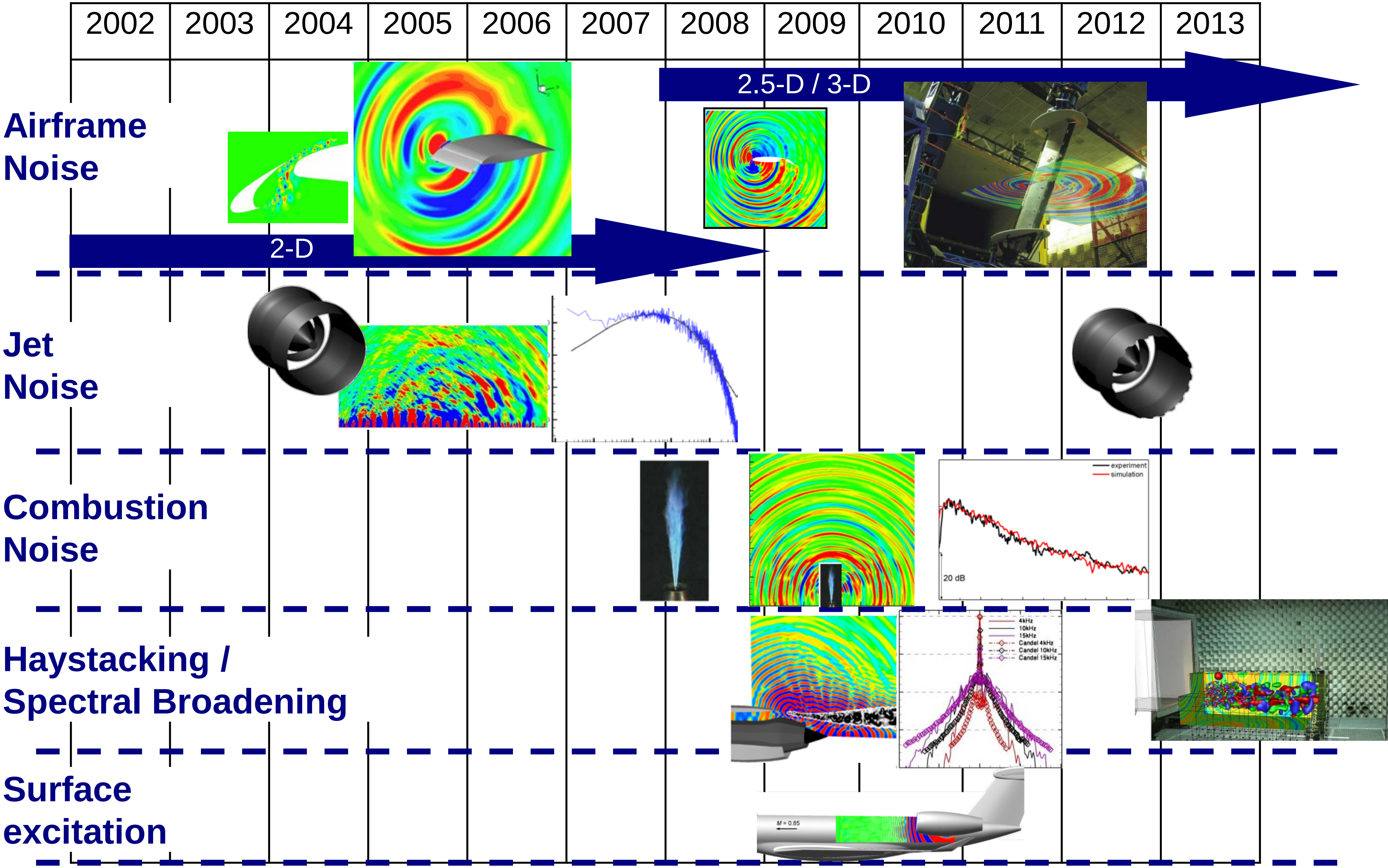

Statistical Noise Theory (SNT)

Two-point cross-correlatiion function and sound spectrum

Spectrum of p'

Acoustic propagation

$$\boxed{S(\boldsymbol{x},\omega)} = \iiint \boxed{\widehat{G}(\boldsymbol{x},\boldsymbol{x}_1,\omega)\,\widehat{G}^*(\boldsymbol{x},\boldsymbol{x}_1+\boldsymbol{r},\omega)} \times$$

This one is modeled empirically, i.e. based on measured shapes

$$\times \boxed{\langle q_s\left(\boldsymbol{x}_1,t\right) q_s\left(\boldsymbol{x}_1+\boldsymbol{r},t+\tau\right)\rangle} e^{i\omega\tau}\mathrm{d}\tau\;\mathrm{d}^3\boldsymbol{x}_1\mathrm{d}^3\boldsymbol{r}$$

Two-point cross-correlation of turbulent source

DLR

Statistical Noise Theory as the Basis of Stochastic Source Models

Historical Overview

1952 **Lighthill**
Ribner

1977 **Mani, Balsa & Gliebe**

1992 **Khavaran, Krejsa & Kim**

1999 **Tam & Auriault**
2003 **Harper-Bourne**
2004 **Morris & Bouluriaan**

2005 **Khavaran, Bridges & Georgiadis**
2006 **Raizda & Morris**
2010 **Karabasov et al.**

2011 **Leib & Goldstein**

Tam & Auriault 1999*: adjoint LEE (spectral space) + equivalent source vs. Measurements

***AIAA JOURNAL Vol. 37, No. 2, Feb. 1999**

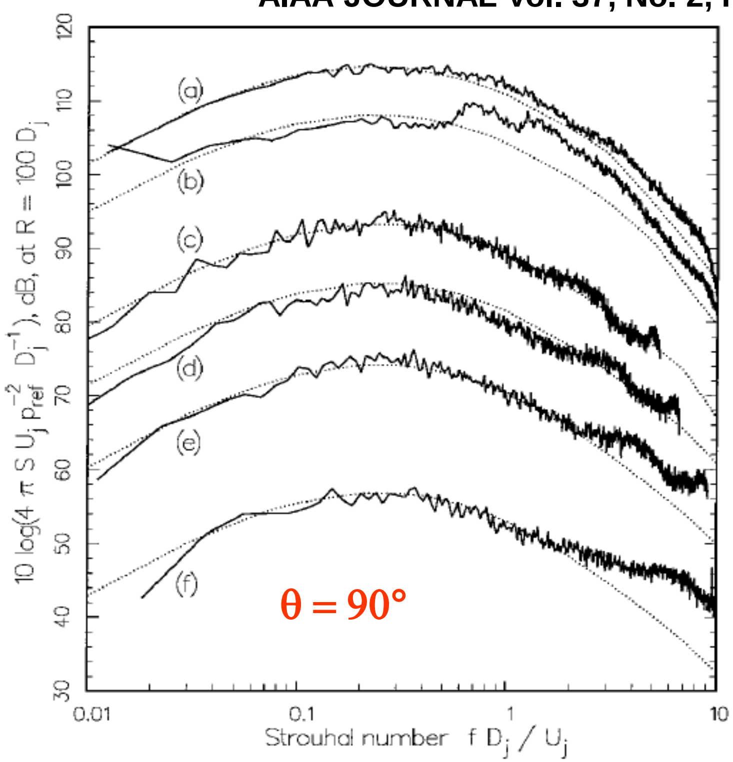

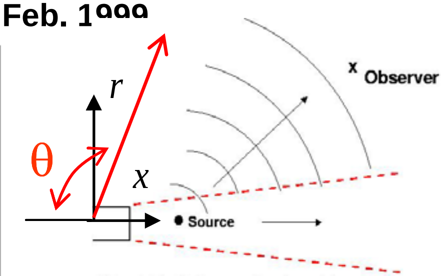

Quintessence: SNT are capable to capture general broadband trends quite well (but: for simple jet nozzles and mainly under 90°)

——, experiments, ... , Tam & Auriault model.

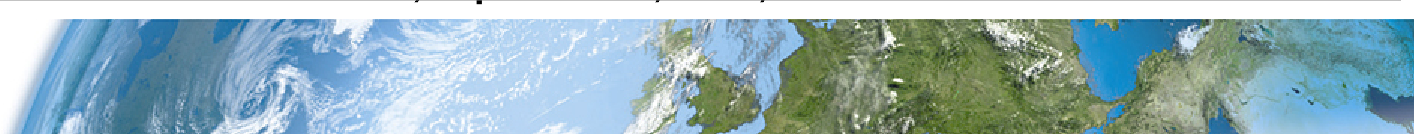

Stochastic Methods: SNT solved in time w. state-of-the-art CAA

Principle

- Realize synthetically fluctuating source with desired two-point statistics

$q_s\left(\boldsymbol{x},t\right) =$

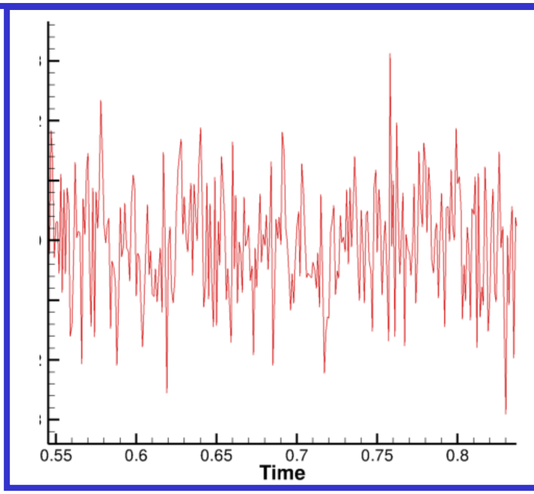

$\langle q_s q_s \rangle =$

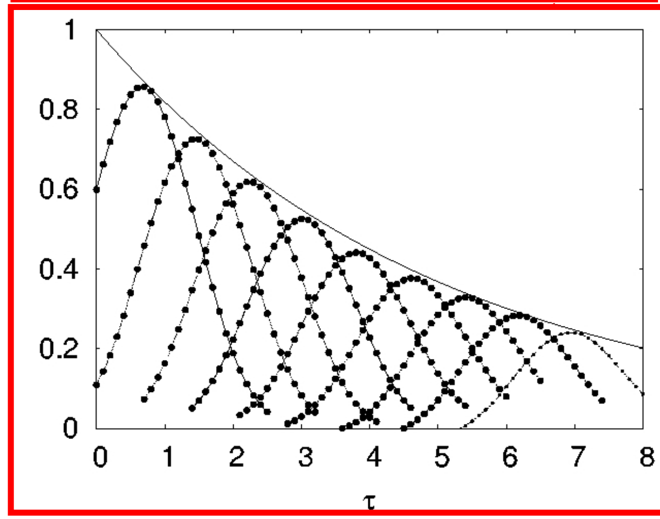

- Solve acoustic analogy with fluctuating source in the time domain

$$\boxed{\text{Acoustic propagation (wave operator)}}\;\boxed{p'} = \boxed{q_s}$$

- Sample pressure data and compute sound spectra
- Sound spectrum corresponds to that of SNT if
    - acoustic propagation model is the same
    - two-point cross-correlation model is identical

'Don't believe it! Prove it to me!!!!'

DLR

Stochastic Methods in CAA

Historical Overview

2012	**Cozza et al.**	**→ *ESDF*, cross-correlation method**
2011	**Dieste & Gabard**	**→ Cyclostationary turbulence, *RPM***
2011	**Casalino et al.**	**→ *SNGR* type of model applied to NACA0012 trailing edge noise**
2010	**Dieste & Gabard**	**→ Evolving turbulence model, *RPM***
2009	**Siefert & Ewert**	**→ Sweeping evolving turbulence model and faster filter for *FRPM***
2009	**Dieste & Gabard**	**→ Random particle method, cross-correlation model**
2007	**Ewert**	**→ Fast Random Particle-Mesh Method (*FRPM*) (increased efficiency)**
2006	**Ewert**	**→ Random Particle-Mesh Method (*RPM*) - cross-correlation model for CAA**
2005	**Ewert et al.**	**→ *SDF*, first stochastic cross-correlation model for CAA**
2004	**Bauer et al.**	**→ *SNGR* trailing edge noise prediction operational**
2003	**Billson et al.**	**→ Langevin equation based evolving turbulence for *SNGR***
2000	**Kallitzin et al.**	**→ Attempt to model trailing edge noise with *SNGR***
1996	**Bailly et al.**	**→ Stochastic Noise Generation and Radiation (*SNGR*) approach – Fourier space based**
1994	**Bechara et al.**	**→ Fourier space based approach for CAA**
⋮	⋮	⋮
1970	**Kraichnan**	**→ Spatial Fourier mode model in moving frame**

DLR

(F)RPM synthetic turbulence generator of DLR

2-D Test problem and comparison FRPM vs. analytical solution

- Verification of FRPM with analytical solution and absolute levels
- CAA-Domain: $u_0=0$ (sound propagation in medium at rest)
- FRPM Patch: $u_c=0.5$
  - Source variance distribution defined by cosine function
  - Tam & Auriault source model with exponential temporal decorrelation
- Comparison with analytical far-field spectrum

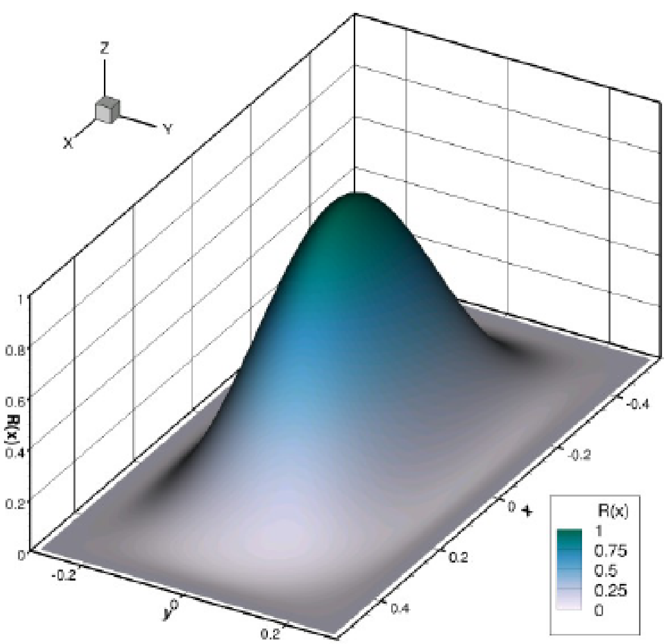

Source patch with source distribution

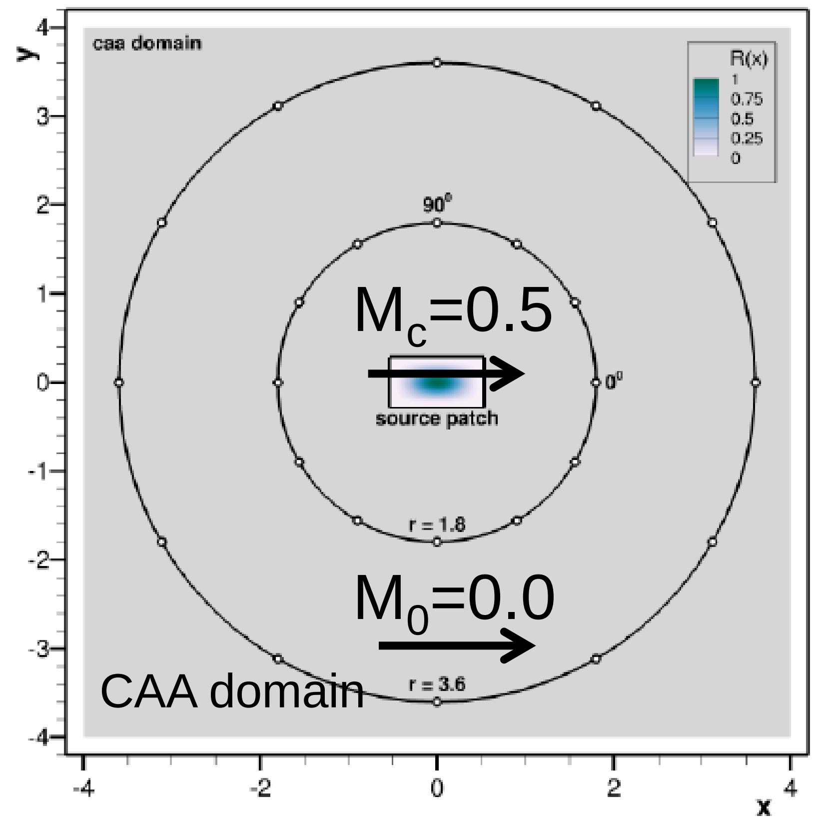

2-D Test Problem, FRPM based Solution

Evaluation of FRPM cross-correlation

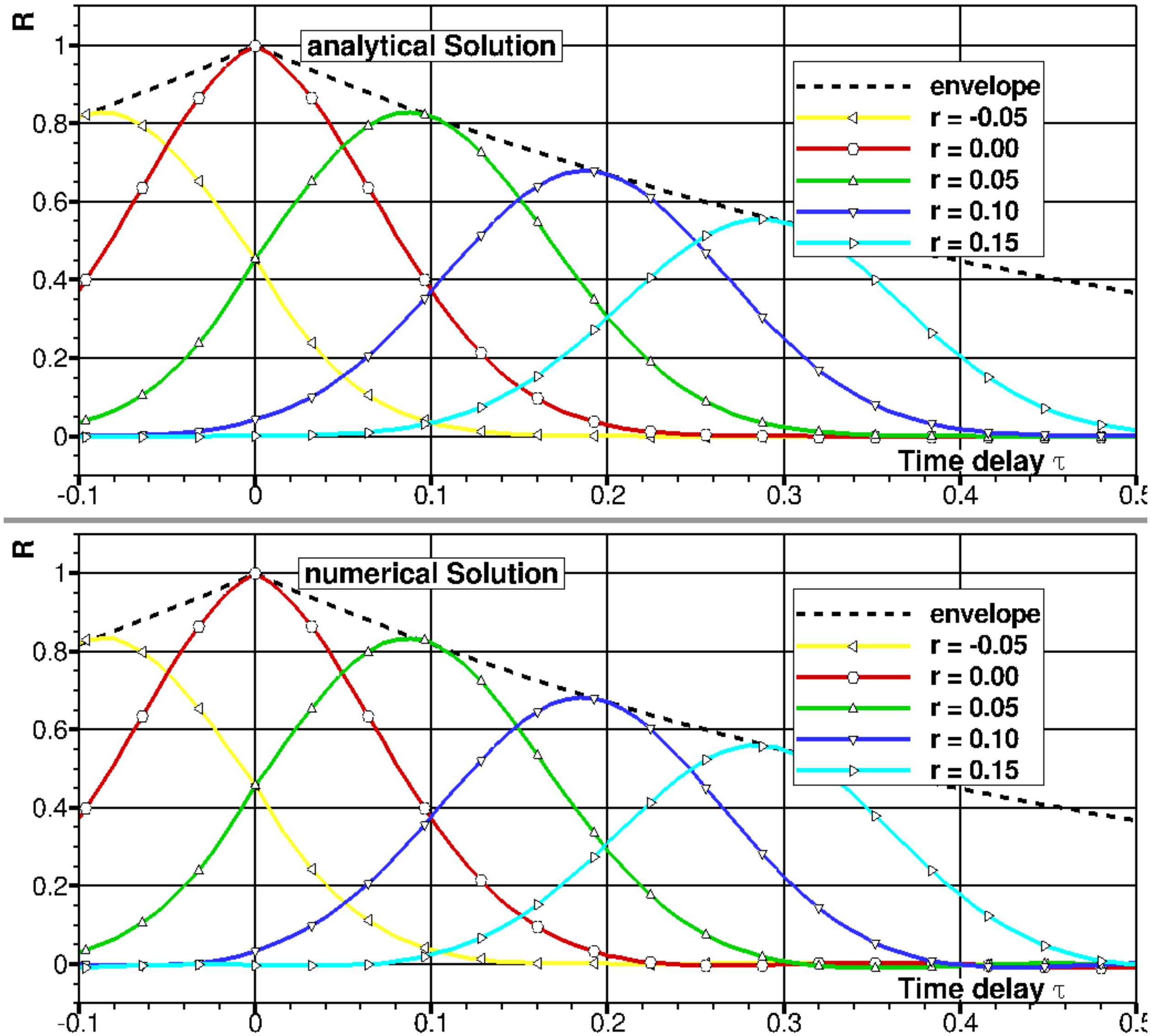

- **time-scale**

$$\frac{u_c \tau_s}{l_s} \approx 4.0$$

2-D Test Problem, FRPM based Solution

Evaluation of FRPM cross-correlation

verified

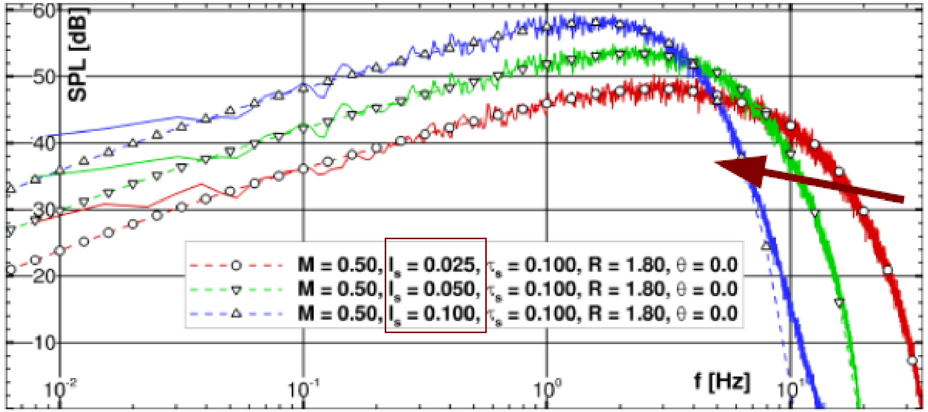

Length scale variation, polar angle θ=0° (downstream direction)

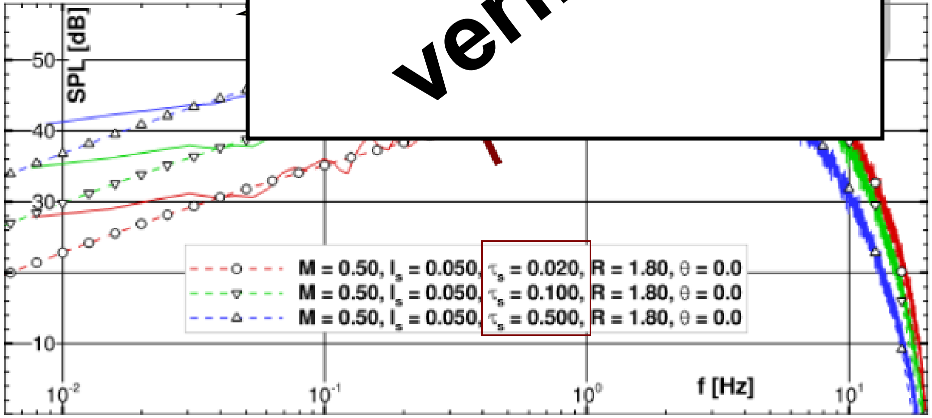

Time scale variation, polar angle θ=0° (downstream direction)

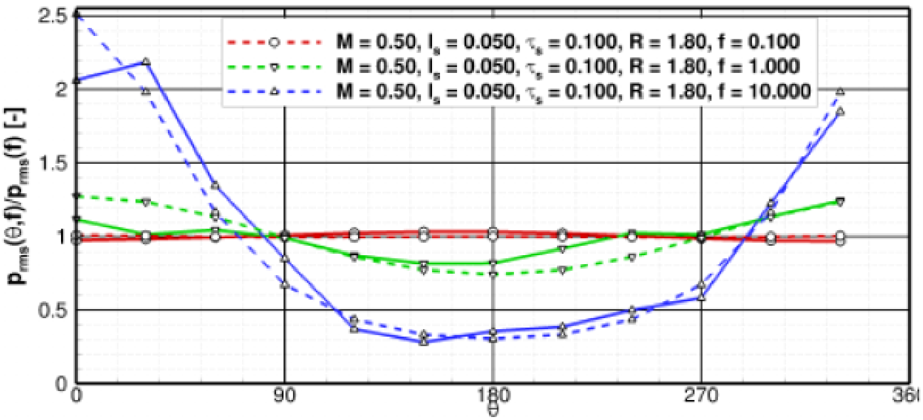

Radial distance R=1.8

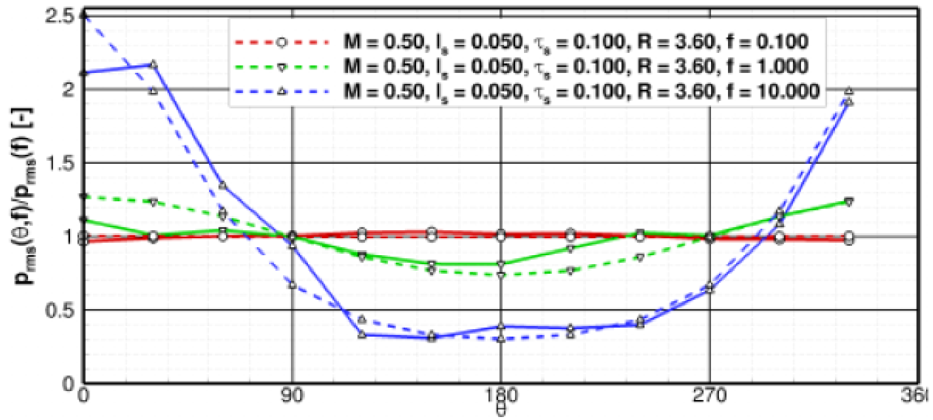

Radial distance R=3.6

Directivity, M_c=0.5, l=0.05, τ_s=0.1, R=1.8 and R=3.5

——, FRPM+CAA, …… , Analytical

Slat Noise Simulations

Slat noise and slat noise reduction measures

1. Slat-cove cover (filler) to reduce kin. energy of turbulence at the TE

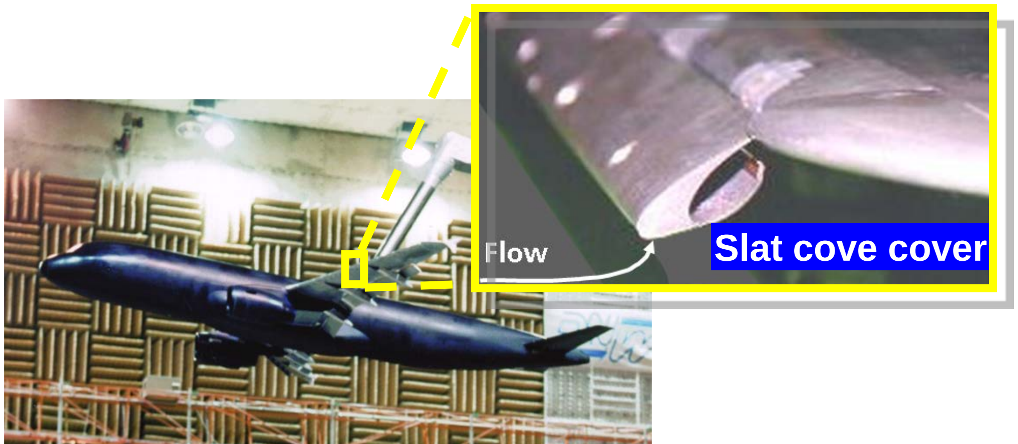

3-dB noise reduction 1:7.5 scale A/C model (Dobrzynski et al. AIAA 98-2337)

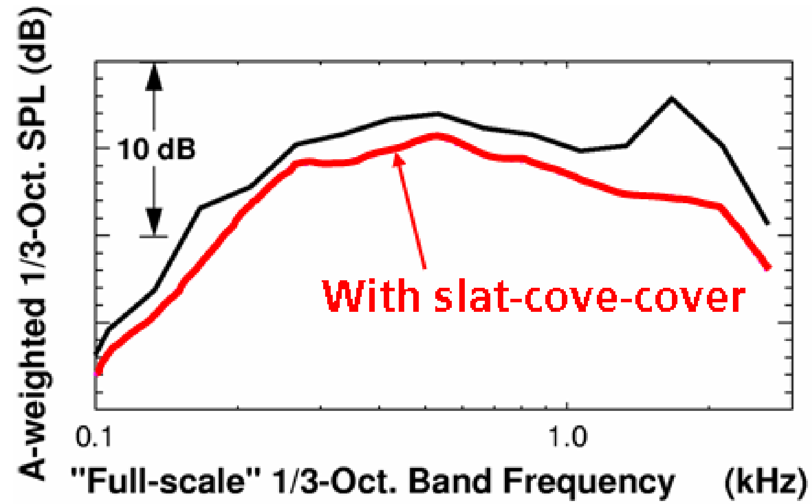

2. Determine low noise slat setting with acceptable loss in lift

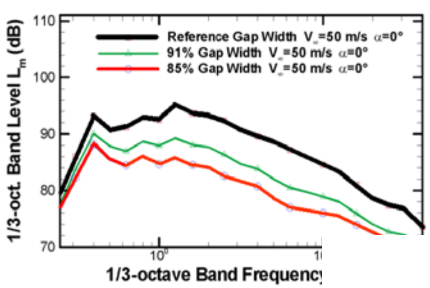

M. Pott-Pollenske

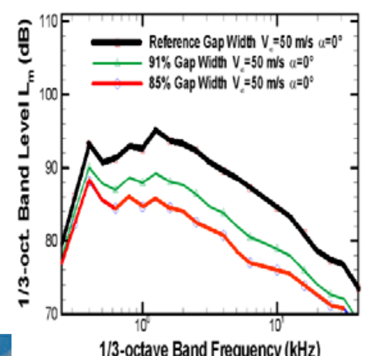

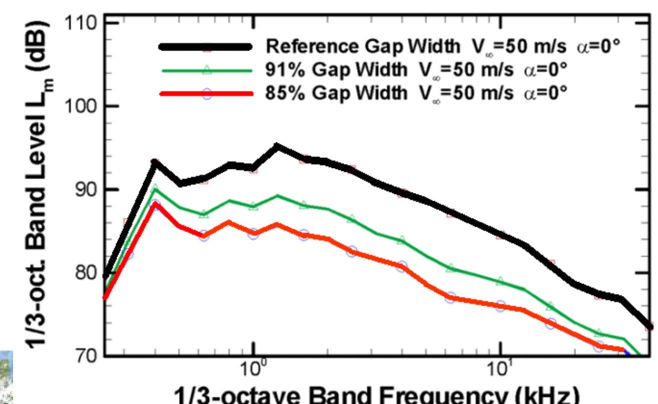

DLR

Slat Noise Simulations

Slat cove filler effect on broadband noise (German national project FREQUENZ)

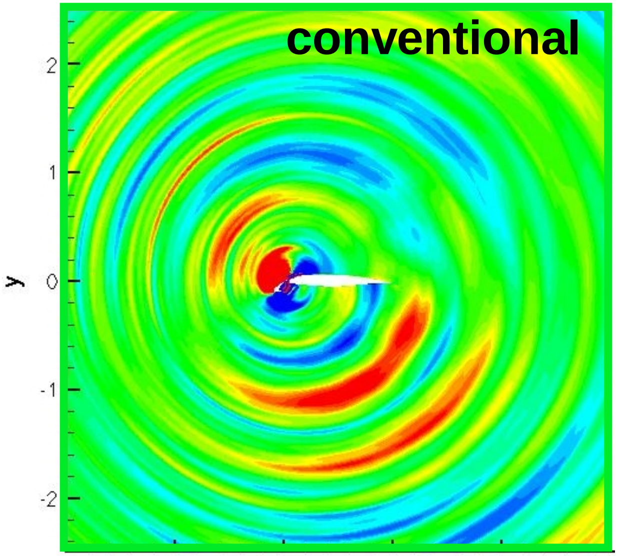

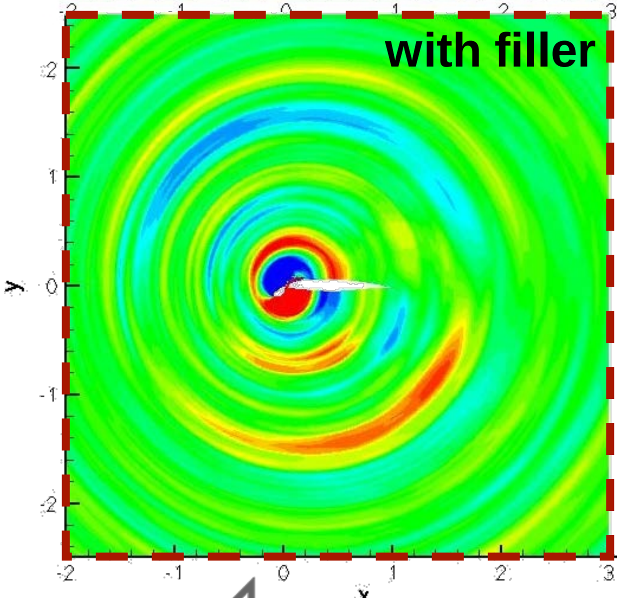

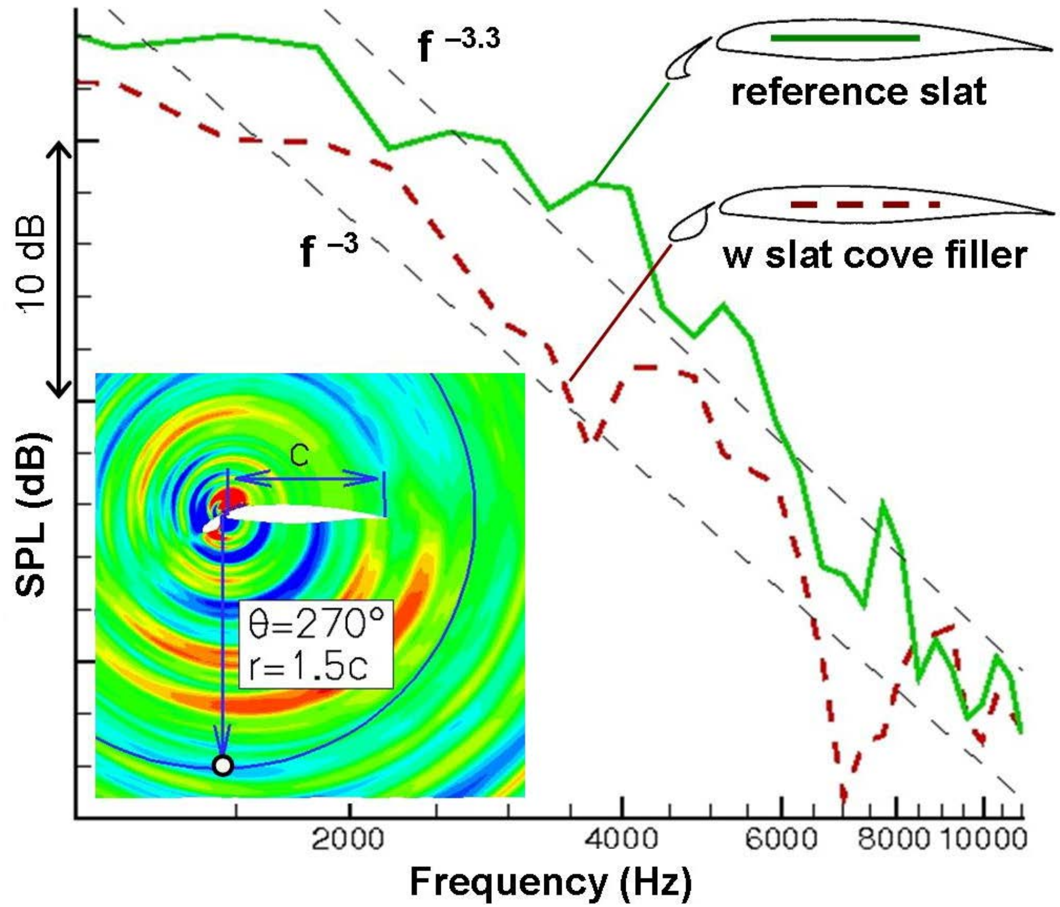

CFD (RANS): TAU (Airbus)
CAA: PIANO (DLR)

Slat Noise Simulations

Slat gap variation and experimental validation (EU TIMPAN)

- *Narrow band spectra at 287° (normal to shear layer)*
- *Prediction made prior to measurements*
- *Prediction based on 0.2sec real time sample, yielding lower frequency resolution and/or larger wiggles*

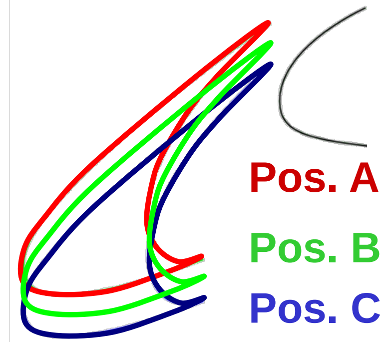

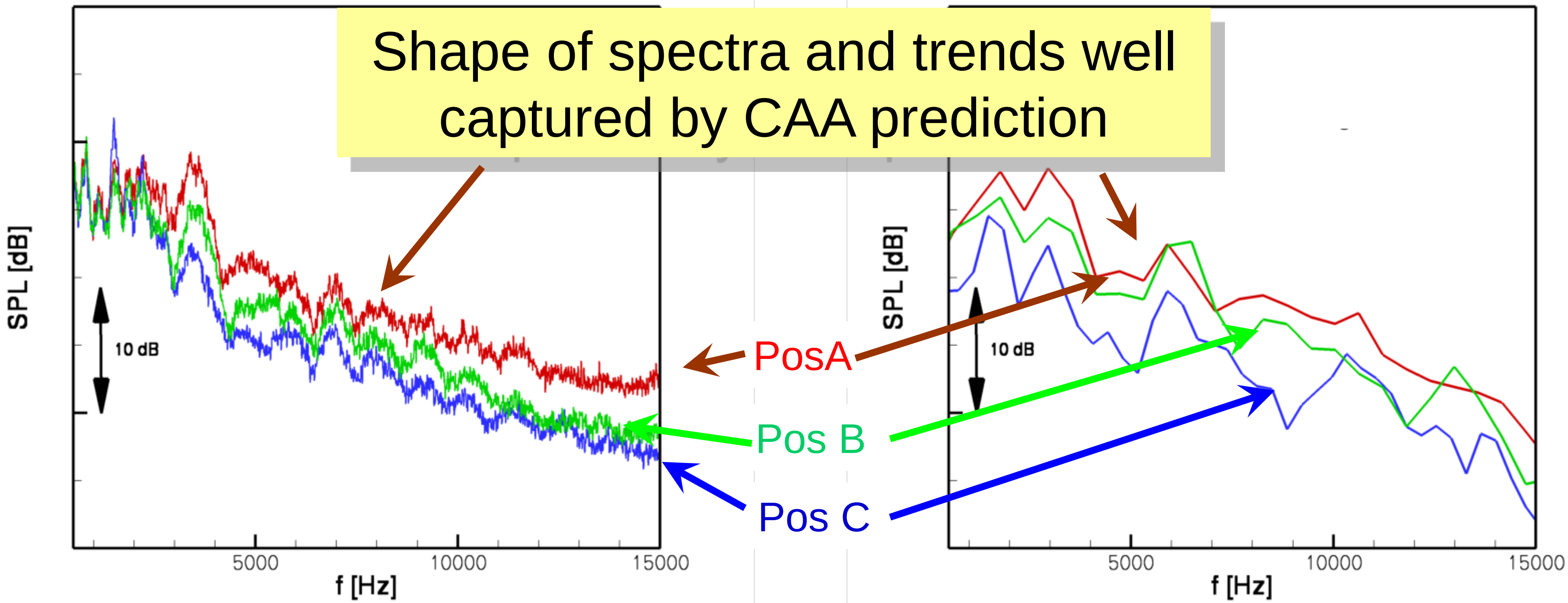

Narrow Band Spectra theta=287° (below airfoil)

Airframe noise of high lift airfoil 30P30N

-Comparison of stochastic approach (PIANO) with other groups

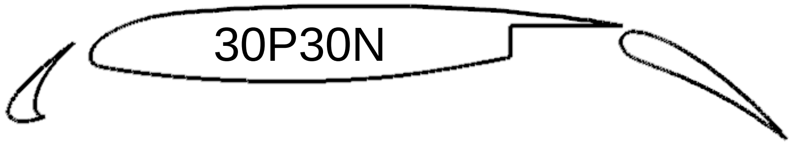

p_{rms}

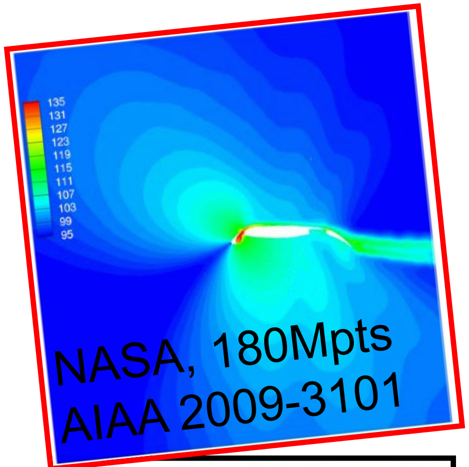

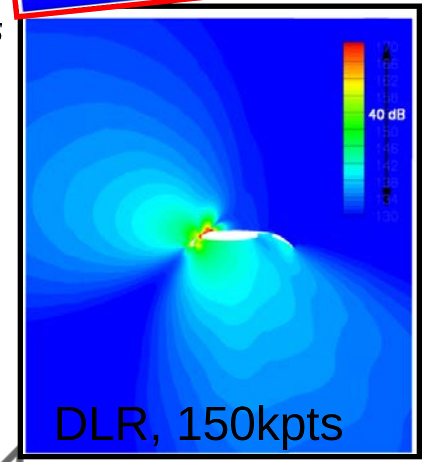

flow: TAU
sound: PIANO

290° w.r.t. flow

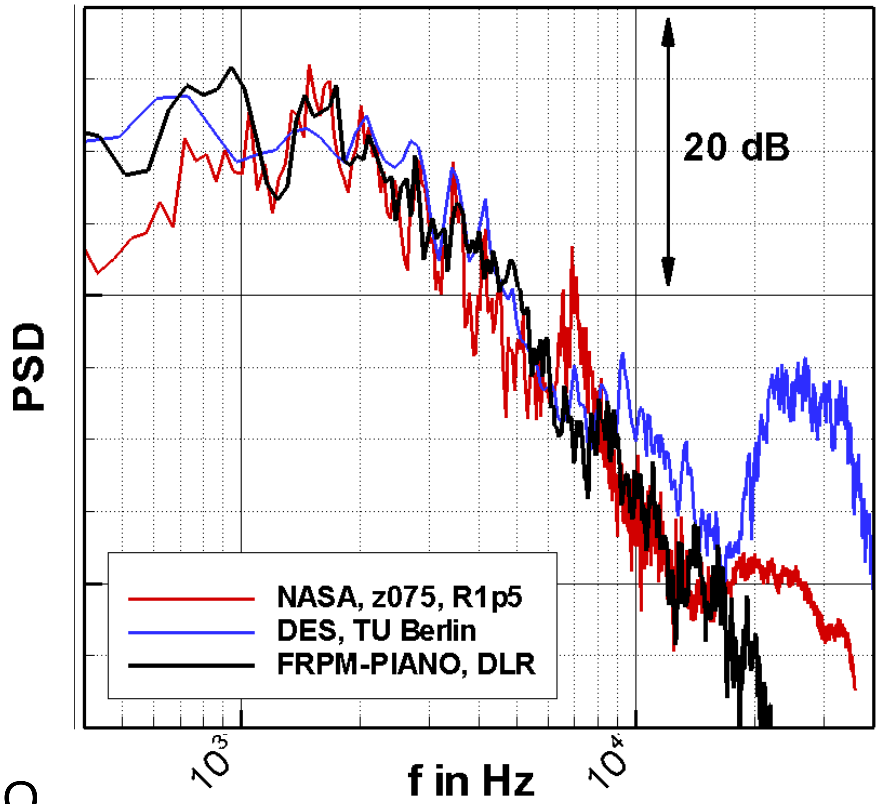

Slat Noise Simulations

Further predictions, 30P30N high-lift airfoil


MD (Boeing) 30P30N profile

- Reynolds number effect (Re=1.7e6 vs. 10e6, Aeronext)
- Extension of CAA simulation capability to unstructured meshes (DG)
- Comparison with scale resolving simulation
- 3-D Sweep effect
- Validation with low Re-number measurements (EU Valiant, Re=7e5)
- Validation with high Re-number measurements (OPENAIR, FTEG, Re=5e6)
- Source anisotropy and modeling effects
- Understanding of source mechanisms?

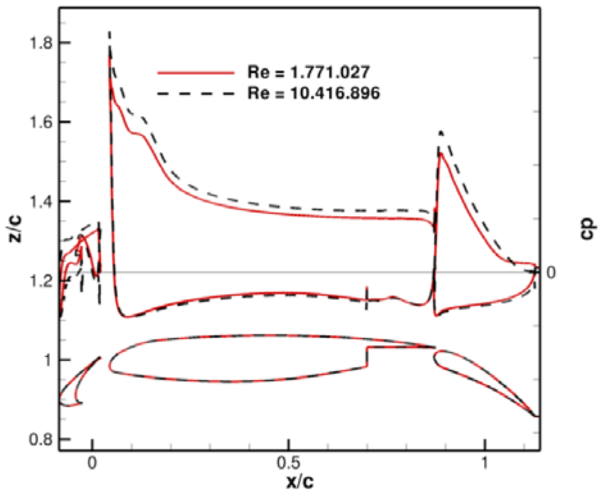

Re-no. effect on Cp distribution from RANS

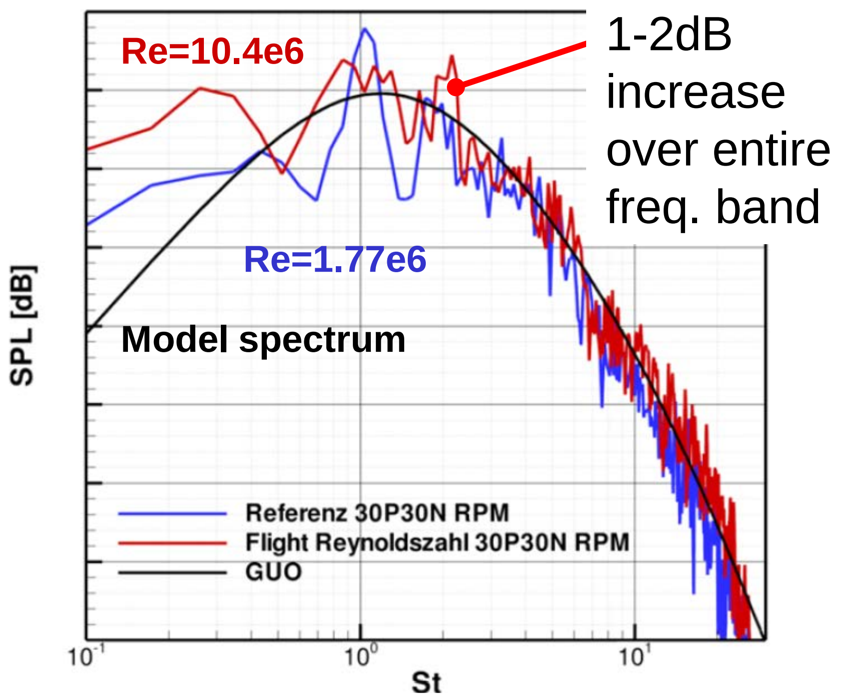

CAA predicted effect on spectrum and comparison with model spectrum of Guo

DLR

Practical application of the DGM

McDonnell Douglas (now Boeing) 30P30N profile

Slat noise of 30P30N high-lift airfoil configuration [Bauer 2011]

L = 0.46 m, Ma_∞ = 0.17, $Re \approx$ 1 700 000, α = 4°
spatial discretization of APE (2D) through a DGM using
Lagrange polynomials of degree $p=3$
unstructured, triangular DG grid: E = 58.774, $f_{limit} \approx$ 15 kHz:

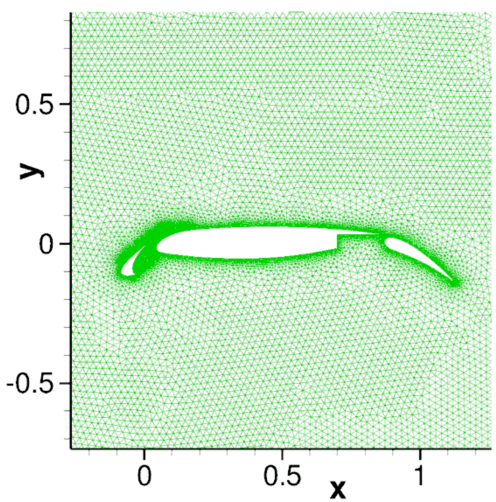

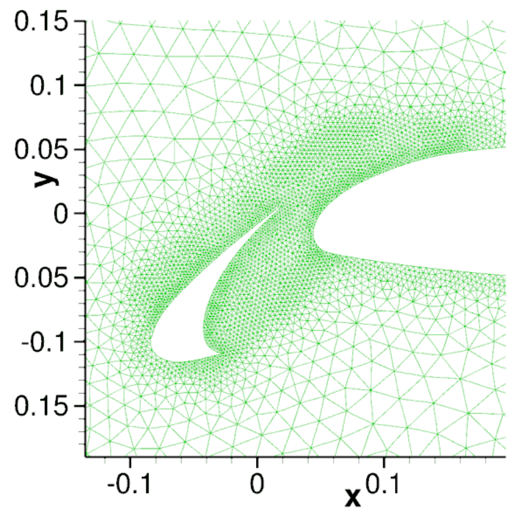

Advantages:

- **local** grid refinement
- **automatic** generation (e.g. with CENTAUR)
- **no** grid **singularities**

Slat Noise Simulations

Comparison of noise predictions 30P30N (r=1.5c)

- DDES+FW-H, TU-B, 3-D, 30Mpts
- RANS/LES+FW-H NASA, 3-D, 62Mpts
- CAA+FRPM 2-D (DLR), 150kpts

Re = 1.7×10^6
A = 4°
Sweep: 0°

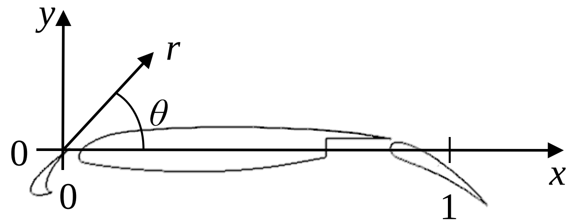

MD (Boeing) 30P30N profile

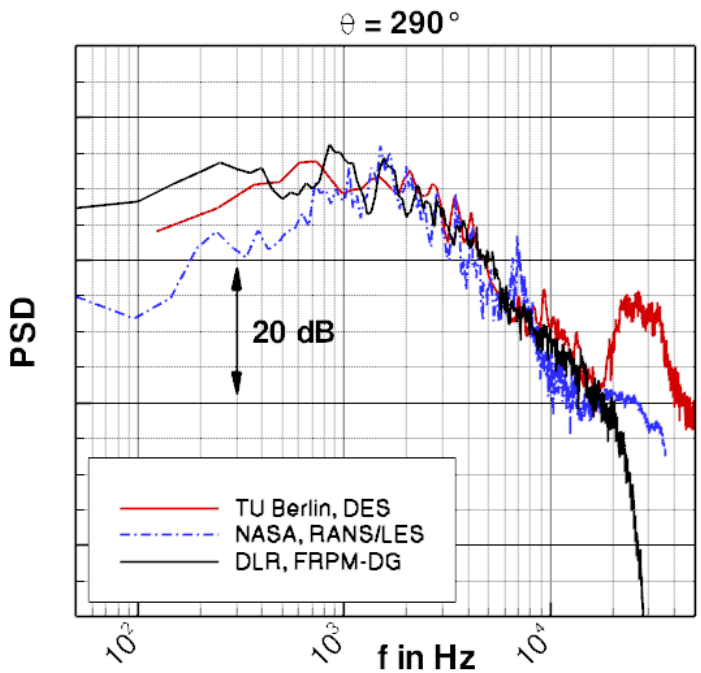

good agreement between 1 and 10 kHz, similar trend

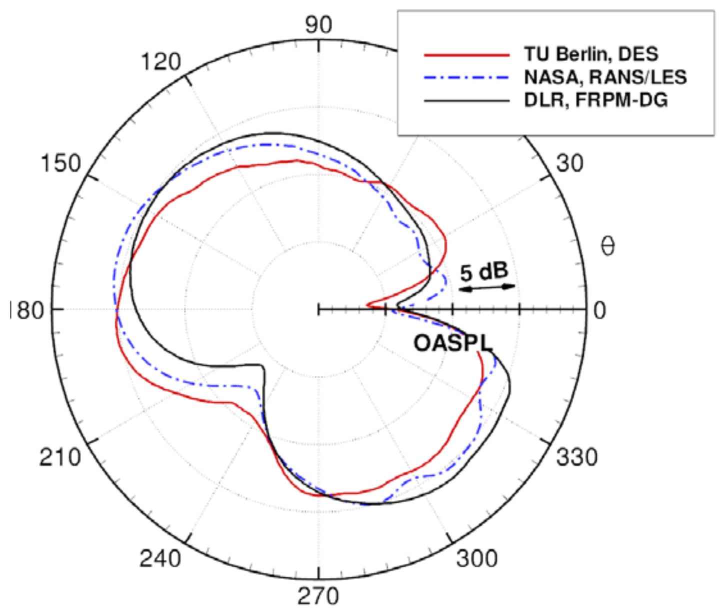

good agreement, all approaches predict minima under $\theta \approx 0°$ and $\theta \approx 225°$

- potential reasons for deviations: vortex shedding from blunt slat upper TE (TU Berlin)

Bauer 2012 & Dierke 2010, Aeronext (LuFo, German)

flow: TAU / sound: DISCO

Slat Noise Simulations

Efficiency of slat noise simulations, DGM vs. PIANO, single processor tests

- comparison of computation times DG Method (DISCO) ⇔ FD Method (PIANO):
  - same settings in PIANO and DISCO:
    - 300.000 time steps, $dt = 1.0E\text{-}04 \rightarrow t_{end} = 30$
    - single 2.8 GHz processor, compilers: gfortran, Intel
  - grids: 653 776 points (PIANO), 587 740 nodes (DISCO)

PIANO-FRPM gfortran / intel
77h / 90h

DISCO-FRPM, global dt	DISCO-FRPM, local dt
59h	**18h**

FRPM only
9h

Uniform (global) time stepping — Non-uniform time stepping

- **DG method practically as efficient as finite-difference method (PIANO)** on single processor

Bauer 2012

Slat Noise Simulations

Spectral results of stochastic results of slat case VALIANT vs. measurement*

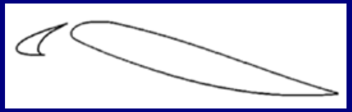

- No tripping of high-lift model in experiments
- Experimental spectra show distinct tones
- BBN noise trends well captured
- But: tones not captured by BBN stochastic approach
- Characteristic slat noise spectrum of Guo (BBN) (black curve):

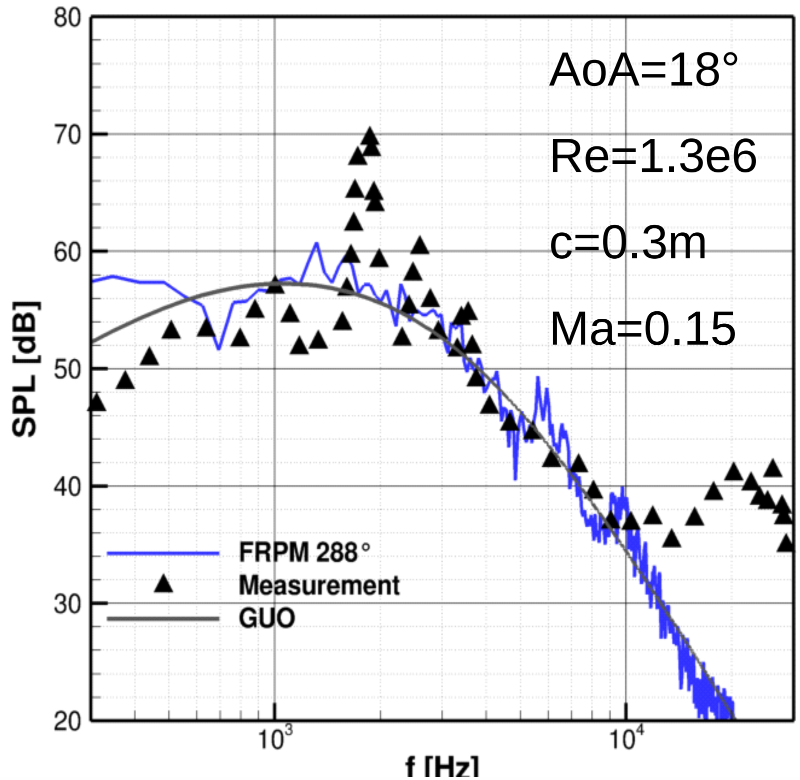

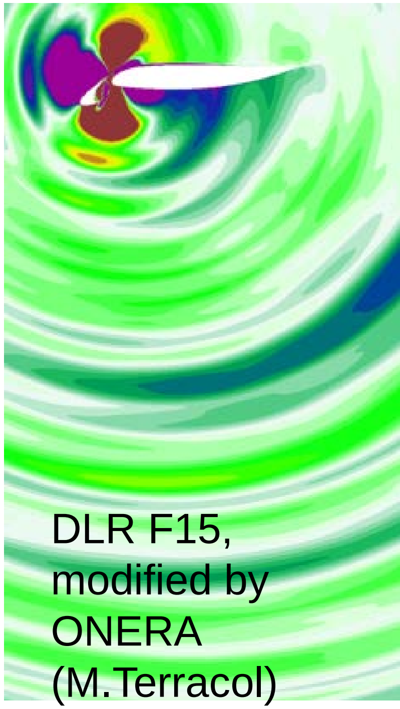

$$F(f,M) = \frac{M^2 c_s}{c_0} \frac{St^2}{(1+\mu_0^2 St^2)(1+\mu_1^2(1+M)^2 St^2)(1+\mu_2^2 M^2 St^2)(1+\mu_3 M St)}$$

$$\mu_1 = 0.26, \quad \mu_2 = 1.0399, \; \mu_3 = 1.78 \text{ and } \mu_4 = 2.2.$$

Summary and Conclusion

- Discussion of the different numerical approaches applied at DLR
- Surface integral methods based on FW-H integrals include simplified propagation physics
  - If not all parts of the airframe are entirely wrapped-up -> BEM Problem
  - Efficient realization (general simulation capability) for realistic airframe sizes and interesting frequencies via Fast Multipole BEM
  - Non-uniform flow effects sometimes important -> volume resolving CAA methods necessary for resolving them
- DNC simulation capability based on DRP scheme and NLPE formulation currently implemented and tested
- Design (fast prediction) methods implemented based on linear perturbation equations (APE) plus stochastic sound sources
- For high-lift systems gives qualitatively good prediction of broadband spectra comparable with measurements and scale resolving simulation
- Stochastic tools provide only broadband part of spectra (no tones)
- DGM promising tool for acoustic propagation purposes based on linear governing equations

Thank you for your attention!

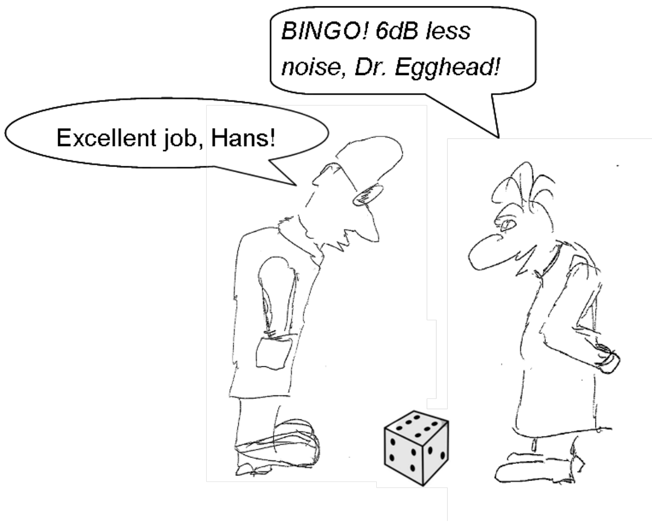

Thank you for your attention!